GEOCHEMICAL EVOLUTION OF ACIDIC GROUND WATER AT A RECLAIMED SURFACE COAL MINE IN WESTERN PENNSYLVANIA[1]

by

Charles A. Cravotta III[2]

Abstract. Concentrations of dissolved sulfate and acidity in ground water increase downflow in mine spoil and underlying bedrock at a reclaimed surface coal mine in the bituminous field of western Pennsylvania. Elevated dissolved sulfate and negligible oxygen in ground water from bedrock about 100 feet below the water table suggest that pyritic sulfur is oxidized below the water table, in a system closed to oxygen. Geochemical models for the oxidation of pyrite (FeS_2) and production of sulfate (SO_4^{2-}) and acid (H^+) are presented to explain the potential role of oxygen (O_2) and ferric iron (Fe^{3+}) as oxidants. Oxidation of pyrite by O_2 and Fe^{3+} can occur under oxic conditions above the water table, whereas oxidation by Fe^{3+} also can occur under anoxic conditions below the water table. The hydrated ferric-sulfate minerals roemerite [$Fe^{2+}Fe_2^{3+}(SO_4)_4 \cdot 14H_2O$], copiapite [$Fe^{2+}Fe_4^{3+}(SO_4)_6(OH)_2 \cdot 20H_2O$], and coquimbite [$Fe_2(SO_4)_3 \cdot 9H_2O$] were identified with FeS_2 in coal samples, and form on the oxidizing surface of pyrite in an oxic system above the water table. These soluble ferric-sulfate "salts" can dissolve with recharge waters or a rising water table releasing Fe^{3+}, SO_4^{2-}, and H^+, which can be transported along closed-system ground-water flow paths to pyrite reaction sites where O_2 may be absent. The Fe^{3+} transported to these sites can oxidize pyritic sulfur. The computer programs WATEQ4F and NEWBAL were used to compute chemical speciation and mass transfer, respectively, considering mineral dissolution and precipitation reactions plus mixing of waters from different upflow zones. Alternative mass-balance models indicate that (a) extremely large quantities of O_2, over 100 times its aqueous solubility, can generate the observed concentrations of dissolved SO_4^{2-} from FeS_2, or (b) under anoxic conditions, Fe^{3+} from dissolved ferric-sulfate minerals can oxidize FeS_2 along closed-system ground-water flow paths. In a system open to O_2, such as in the unsaturated zone, the aqueous solubility of O_2 is not limiting, and oxidation of pyrite by O_2 and Fe^{3+} accounts for most SO_4^{2-} and Fe^{2+} observed in acidic ground water. However, in a system closed to O_2, such as in the saturated zone, O_2 solubility is limiting; hence, ferric oxidation of pyrite is a reasonable explanation for the observed elevated SO_4^{2-} with increasing depth below the water table.

Additional Key Words: acid mine drainage; pyrite oxidation; ground-water flow modeling; sewage sludge; ferric-sulfate minerals.

Introduction

Acidic ground water and acid mine drainage (AMD) can result from the accelerated oxidation of iron-sulfide minerals, such as pyrite, that are exposed during coal mining. The acidic water typically contains large concentrations of sulfate, iron, and other solutes that are dissolved from the reactive minerals in the mined coal and overburden. AMD can degrade the aquatic habitat and the quality of water supplies.

The U.S. Geological Survey (USGS), in cooperation with the Pennsylvania Department of Environmental Resources (PaDER) and with help from a private mining company, conducted an investigation of the factors affecting water quality at a surface-coal mine in western Pennsylvania that was reclaimed partly by application of composted municipal sewage sludge. Incorporation of sewage sludge with mine spoil creates a nutrient-and-moisture-rich medium that supports reestablishment of vegetation on the disturbed landscape (Sopper and Seaker 1984; Seaker and Sopper 1988a,b). It was hypothesized that the decay of organic matter from the sludge and perennial vegetation would deplete oxygen in recharge waters and thus slow or inhibit acid-forming, pyrite-oxidation reactions in the sludge-reclaimed mine spoil. However, unexpected increases in concentrations of sulfate and acidity were measured in ground water downflow from the sludge-treated mine spoil. Negligible concentrations of dissolved oxygen (DO) suggest that acidic ground water evolves by sequential interactions with pyrite and other minerals under oxygen-limited conditions. This paper (1) reviews geochemical reactions that are likely to produce acidic, mineralized ground water, and (2) evaluates if anoxic conditions limit oxidation of pyrite and production of acid below the water table. Geochemical mass-transfer models are presented to quantify the chemical evolution of water and rock along selected flow paths through the mine spoil and bedrock.

Geochemistry of Acid Mine Drainage

Production of Acid

AMD results from the interactions of oxygen, water, bacteria, and sulfide minerals (Temple and Koehler 1954; Singer and Stumm 1970a,b; Nordstrom et al. 1979; Kleinmann et al. 1980; Cathles 1982; Nordstrom 1982). Pyrite (FeS_2), and less commonly marcasite (FeS_2), are the principal sulfur-bearing minerals in bituminous coal (Davis 1981; Hawkins 1984), and because of its wide distribution, pyrite is recognized as the major source of AMD in the eastern United States (Stumm and Morgan 1981, p. 469).

The following overall stoichiometric reactions may characterize the oxidation of pyrite and other iron disulfide minerals exposed to oxygen and water (Stumm and Morgan 1981, p. 470):

$$FeS_2 + 3.5\ O_2 + H_2O \implies Fe^{2+} + 2\ SO_4^{2-} + 2\ H^+, \tag{1}$$

$$Fe^{2+} + 0.25\ O_2 + H^+ \implies Fe^{3+} + 0.5\ H_2O, \tag{2}$$

$$Fe^{3+} + 3\ H_2O \implies Fe(OH)_3 + 3\ H^+. \tag{3}$$
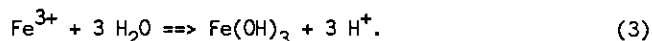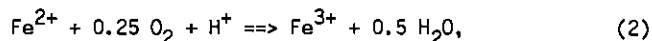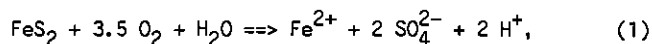
The oxidation of 2 mol of sulfide in pyrite to sulfate (SO_4^{2-}) (reaction 1) consumes 3.5 mol of oxygen (O_2) and releases dissolved ferrous iron (Fe^{2+}) and acid (H^+) into the water. In acidic, aerobic environments, the autotrophic, iron-oxidizing bacteria, _Thiobacillus ferrooxidans_, can catalyze the oxidation of Fe^{2+} to ferric iron (Fe^{3+}) (reaction 2) (Colmer and Hinkle 1947; Colmer et al. 1949; Temple and Colmer 1951; Temple and Delchamps 1953; Temple and Koehler 1954; Singer and Stumm 1970a,b). However, as acid is neutralized, Fe^{3+} tends to hydrolyze forming relatively insoluble ferrihydrite [$Fe(OH)_3$] (reaction 3) (Whittemore and Langmuir 1975). The overall combination of reactions 1 through 3 may be written

$$FeS_2 + 3.75\ O_2 + 3.5\ H_2O \implies$$
$$Fe(OH)_3 + 2\ SO_4^{2-} + 4\ H^+. \tag{4}$$
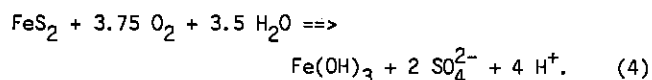
In reaction 4, 3.75 mol of oxygen are consumed to oxidize 1 mol of pyrite and to produce 2 mol of sulfate, 4 mol of acid, and 1 mol of ferrihydrite.

However, other iron minerals, especially ferric-sulfate compounds may form in addition to, or instead of, ferric-oxyhydroxide compounds in acidic weathering environments (Nordstrom et al. 1979; Nordstrom 1982; Karanthanasis et al. 1988, 1990). For example, roemerite may form by the oxidation of pyrite

$$3\ FeS_2 + 11\ O_2 + 16\ H_2O \implies$$
$$Fe^{2+}Fe_2^{3+}(SO_4)_4 \cdot 14H_2O + 2\ SO_4^{2-} + 4\ H^+. \tag{5}$$
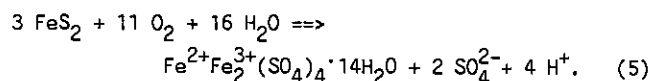
The oxidized minerals roemerite [$Fe^{2+}Fe_2^{3+}(SO_4)_4 \cdot 14H_2O$], copiapite [$Fe^{2+}Fe_4^{3+}(SO_4)_6(OH)_2 \cdot 20H_2O$], and coquimbite [$Fe_2(SO_4)_3 \cdot 9H_2O$] (Palache et al. 1951, p. 520, 532, 623) were identified with pyrite in high-sulfur coal samples collected for this investigation (see discussion of mineralogy below). These hydrated ferric-sulfate salts are highly soluble (Nordstrom 1982) and probably are produced above the water table. They can form in situ, as efflorescences, by the oxidation of iron-sulfide minerals in dewatered, cleated coal seams and (or) in stockpiled or reclaimed overburden. They also can be

precipitated from oxidizing and evaporating iron-and-sulfur-rich solutions at AMD discharge zones or at the capillary fringe in the unsaturated zone (similar to mode of formation of caliche). Such minerals are not likely to be produced below the water table by the oxidation of pyrite, because extreme concentrations of acid, iron, and sulfate are required (D. K. Nordstrom, U.S. Geological Survey 1991, written commun.); however, Baker (1971) reported the presence of ferric sulfate and hydroxide on biologically oxidized, submerged pyrite surfaces that were analyzed under about 0.1 inches (in) of water.

AMD also can form in the absence of O_2. Relatively small amounts of DO may be available below the water table, where O_2 solubility, diffusion, microbial consumption, and oxidation reactions limit the supply of the reactant (Champ et al. 1979; Jaynes et al. 1984a,b). However, Fe^{3+} produced by T. ferrooxidans may oxidize the sulfur in pyrite (Temple and Delchamps 1953)

$$FeS_2 + 14\ Fe^{3+} + 8\ H_2O ==>$$
$$15\ Fe^{2+} + 2\ SO_4^{2-} + 16\ H^+. \qquad (6)$$
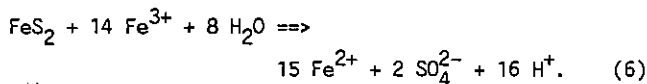
Kinetic data suggest that Fe^{3+} is the direct oxidant of pyrite in oxic and anoxic acid systems (Garrels and Thompson 1960; Singer and Stumm 1970a,b; McKibben and Barnes 1986; Moses et al. 1987).

The storage of Fe^{3+} in the unsaturated zone and its subsequent release into ground water is an important aspect of pyrite oxidation below the water table. For example, as the water table rises or as recharge waters percolate through the mine spoil to the water table, previously formed ferric minerals may be transported or decompose releasing Fe^{3+} into ground water and thus providing an oxidant for pyrite. Barnes and Clarke (1964) suggested that because of the absence of DO and limited solubility of Fe^{3+}, O_2 should be discarded as a major reactant in subsurface mine waters and reactions involving only water and minerals should be considered as controls of mine-water quality. Gang and Langmuir (1974) proposed that suspended ferrihydrite colloids could be a source of Fe^{3+} ions

$$FeS_2 + 14\ Fe(OH)_3 + 26\ H^+ ==>$$
$$15\ Fe^{2+} + 2\ SO_4^{2-} + 34\ H_2O. \quad (7)$$
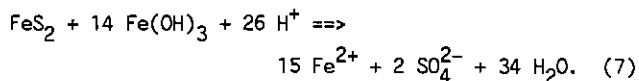
However, the combination of ferrihydrite dissolution and pyrite oxidation neutralizes acid and produces smaller quantities of sulfate than dissolved iron. Although reaction 7 is thermodynamically feasible, $Fe(OH)_3$ is not a likely source of Fe^{3+} because it normally is formed as acidic water is neutralized downflow from its source.

Another source of Fe^{3+} is the soluble, hydrated ferric-sulfate minerals including roemerite, copiapite, and coquimbite, which can form on the surface of pyrite in weathered zones. Jarosite $[(K,Na,H_3O)Fe_3(SO_4)_2(OH)_6]$ is not a likely source of Fe^{3+} ions because it is relatively insoluble in acidic to neutral waters (Nordstrom et al. 1979; Nordstrom 1982). Although Temple and Koehler (1954) and Zajic (1969, p. 101, 114-116) suggested that ferric-sulfate compounds may oxidize pyrite, they did not expand on the significance of these minerals as reactants in coal-mine spoil, especially on their role in the subsurface evolution of acidic ground water under anoxic conditions. For example, the following overall reaction of pyrite and roemerite generates acid without oxygen:

$$FeS_2 + 7\ Fe^{2+}Fe_2^{3+}(SO_4)_4 \cdot 14H_2O ==>$$
$$22\ Fe^{2+} + 30\ SO_4^{2-} + 16\ H^+ + 90\ H_2O. \qquad (8)$$
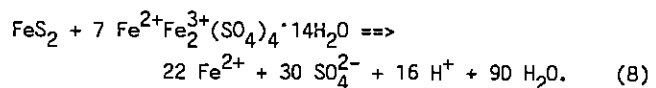
Similar reactions may occur between pyrite and copiapite or coquimbite. One can speculate that attempts to stop AMD formation by excluding O_2 after ferric salts have formed in pyritic mine spoil or coal refuse may not be successful because of the potential for release of stored acid, SO_4^{2-}, and Fe^{3+}.

Neutralization of Acid

Acid from the aqueous oxidation of pyrite can be neutralized by reactions with carbonate, silicate, and hydroxide minerals composing the sedimentary rocks in the coal-bearing sequence. Dissolution of these minerals produces elevated concentrations of dissolved cations such as calcium (Ca), magnesium (Mg), sodium (Na), potassium (K), aluminum (Al), and silicon (Si). The following stoichiometric reactions are presented to show mineral sources of major solutes in AMD and to indicate mass-balance relations employed later for the geochemical interpretation of water-quality data.

The most acid-reactive minerals are the carbonates: calcite $(CaCO_3)$, dolomite $[CaMg(CO_3)_2]$, and siderite $(FeCO_3)$. Carbonates are present in variable quantities as individual mineral grains and as cementing agents in limestone, dolostone, and clastic rocks (sandstone, siltstone, and shale). Dissolution of calcite, dolomite, and other calcium- or magnesium-bearing carbonate minerals neutralizes acid and produces alkalinity (bicarbonate). The dissolution of calcite serves as an example

$$CaCO_3 + H^+ ==> Ca^{2+} + HCO_3^-. \qquad (9)$$
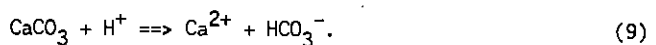
Reaction 9 shows that 1 mol of calcite will neutralize 1 mol of free acid and produce 1 mol each of dissolved calcium and bicarbonate. However, dissolution of siderite, which is a common mineral in coal-bearing strata, and subsequent oxidation and hydrolysis of iron can produce acid as dissolved carbon dioxide and carbonic acid ($H_2CO_3^*$) (Cravotta et al. 1990)

$$FeCO_3 + 0.25\ O_2 + 2.5\ H_2O ==> Fe(OH)_3 + H_2CO_3^*. \quad (10)$$
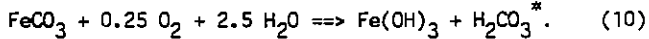
Cations such as Mn, Mg, and Ca commonly substitute for Fe in siderite (Mozley, 1989; Morrison et al. 1990b). The Ca-Mg-carbonate impurities have neutralizing ability similar to calcite and dolomite; however, like Fe (reaction 3), the hydrolysis of Mn ions will generate acid. Thus, because of its variable composition, the acid-forming or neutralizing potential of siderite is difficult to predict.

Dissolution or hydrolysis of aluminosilicate minerals, which predominate in the clastic overburden rocks, neutralizes acid, but also produces dissolved Al, Si, and major cations such as Mg, Na, and K plus solid phases. Complete solution of aluminum-bearing phases can occur under extremely acid conditions; however, quartz (SiO_2) is resistant to sulfuric acid and is a common residual mineral. For example, chlorite may dissolve incongruently producing solid gibbsite [$Al(OH)_3$] and cryptocrystalline or amorphous silica (SiO_2) plus dissolved magnesium

$$Mg_5Al_2Si_3O_{10}(OH)_8 + 10\ H^+ ==>$$
$$2\ Al(OH)_3 + 3\ SiO_2 + 5\ Mg^{2+} + 6\ H_2O. \quad (11)$$
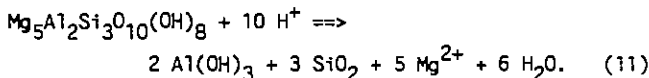
Chlorite commonly contains Fe and Mn substituting for Mg. Dixon et al. (1982) report that the weathering of Fe-chlorite in lignite overburden caused preferential leaching of Mg and Fe relative to Si and Al.

Feldspar may hydrolyze producing kaolinite [$Al_2Si_2O_5(OH)_4$], a common clay mineral, plus dissolved silica, potassium, and sodium

$$2\ K_{0.85}Na_{0.15}AlSi_3O_8 + 9\ H_2O + 2\ H^+ ==>$$
$$Al_2Si_2O_5(OH)_4 + 4\ H_4SiO_4^o + 1.7\ K^+ + 0.3\ Na^+. \quad (12)$$
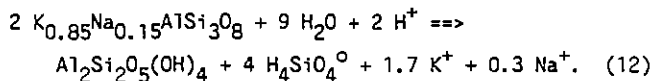
In reaction 12, both K and Na are contained in the feldspar. X-ray diffraction patterns suggest the presence of microcline having this stoichiometry in rock samples collected at the study site (see below).

Elevated concentrations of aluminum are common in AMD because even gibbsite and kaolinite can dissolve in acidic systems (pH less than 4) producing Al^{3+} (Hem

1985), as is shown by the dissolution of kaolinite:

$$Al_2Si_2O_5(OH)_4 + 6\ H^+ ==>$$
$$2\ H_4SiO_4^o + 2\ Al^{3+} + H_2O. \quad (13)$$
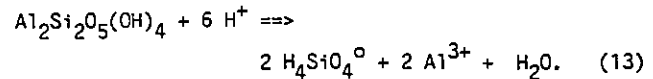
Reaction 13 shows that the dissolution of 1 mol of kaolinite neutralizes 6 mol of H^+ and produces 2 mol of Al^{3+}. Although acid neutralization is desirable, the leaching of aluminum is not desirable because Al^{3+} can be toxic to aquatic biota (Burrows 1977; Baker and Schofield 1982; Burton and Allan 1986), and the hydrolysis of Al^{3+} produces H^+ and buffers pH to be acid.

Mine Location, Geology, and Hydrology

AMD is widespread in the bituminous coal field of western Pennsylvania where surface mining prevails. A surface coal mine in that region was selected for an investigation of ground-water quality. The mine was reclaimed partly by surficial applications of municipal sewage sludge. The PaDER and USGS wanted to determine potential adverse effects on water quality by leaching of heavy metals and nutrients from the sludge. The
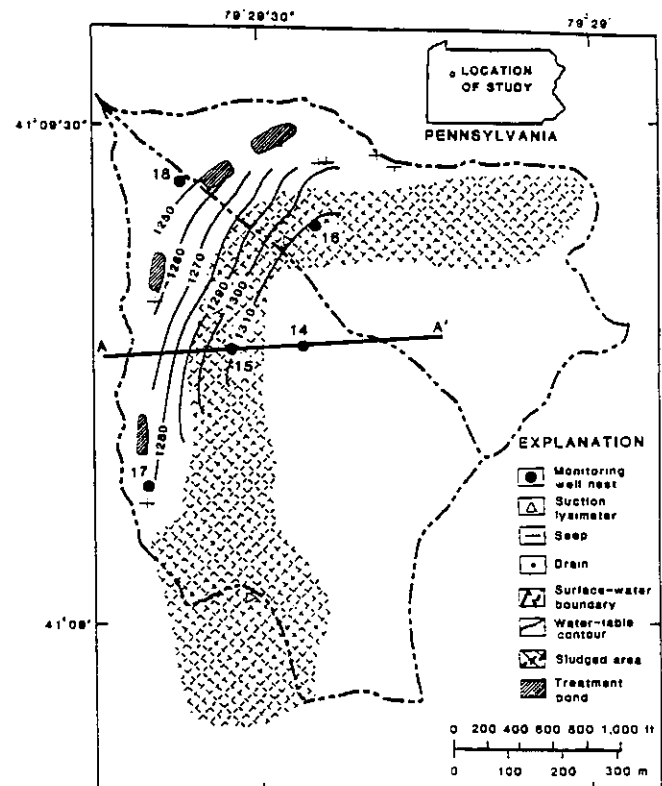
Figure 1.--Location of reclaimed surface coal mine, sewage-sludge-covered area, hydrologic monitoring points, and median water-table configuration. Line A-A' of geologic section in figure 2.

study site also was investigated because AMD had developed during mining and continued to discharge at a number of seeps even though mining and reclamation were completed by enactment of guidelines intended to reduce the effects of mining on the environment.

Mine Location and Description

The study area includes a reclaimed 150-acre surface coal mine about 7 miles (mi) southwest of the city of Clarion in Clarion County, Pennsylvania (see figure 1). The area includes a broad hilltop, surrounded by steep hillsides, and bounded by several small tributaries which flow northward and westward to the Clarion River. Seepage from the mine-spoil banks and outcropping, underlying bedrock flows into these tributaries. Altitudes in the study area range from greater than 1,500 feet (ft) to less than 1,200 ft above sea level.

Prior to 1982, high-volatile bituminous coal of the Allegheny Group was mined by open pit methods.

Overburden was removed using a dragline and bucket, and coal was removed by front-end loader and truck. Because roughly half of the area was mined only for the lower Kittanning coal (hilltop) and the other half only for the upper and lower Clarion coals (hillside), a highwall was created separating upper and lower benches (see figure 2). During mining, the mine was backfilled with overburden and coal waste material, and in 1982 at the completion of mining, the mine spoil was regraded into a terraced topographic configuration corresponding to the upper and lower benches. The average thickness of the mine spoil is about 50 ft on the upper bench and 70 ft on the lower bench.

In the spring of 1986, a mixture of composted wood chips and sewage sludge from Philadelphia wastewater treatment plants (Blickwedel and Linn 1987) was spread at a rate of about 60 dry tons per acre over about 60 acres of the mine-spoil surface on the lower bench (see figures 1 and 2). The sludge-covered spoil composes about 40 percent of the reclaimed area. Berms were constructed along the downslope perimeter of the sludge-
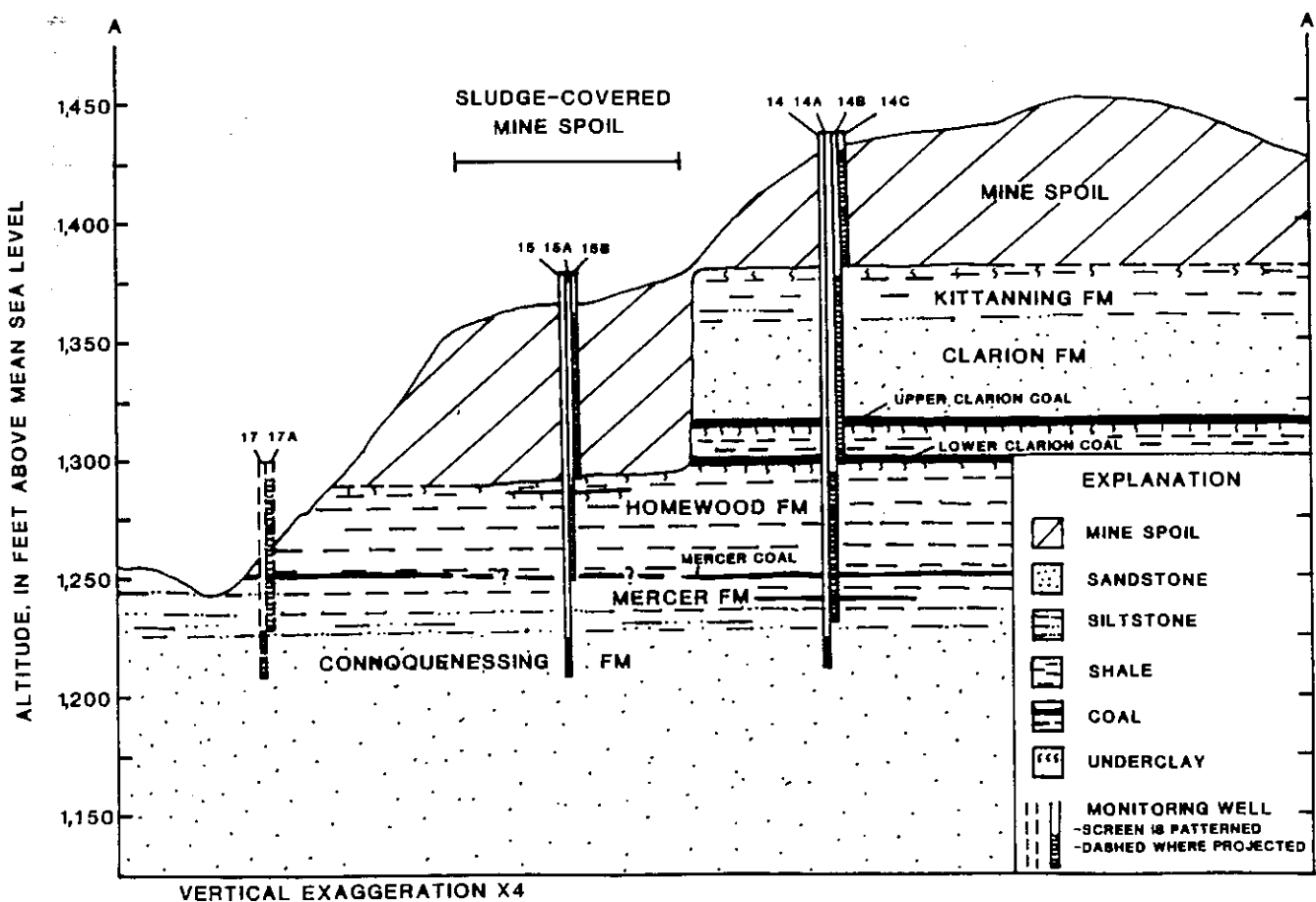
Figure 2.--Geologic section along an east-west traverse through the mine. Line of section shown in figure 1.

treated area to prevent the sludge from eroding (before vegetation could be established) and entering nearby surface water. The composted sludge mixture was not applied on the hilltop, which was planted with pine trees, or on the steep "toe-of-spoil" banks below the berms, which remained barren, erodable, and permeable. In contrast, the sludge-treated areas support lush vegetative growth, which was established within months after seeding with perennial grasses.

Geology, Mineralogy, and Rock Chemistry

The study area is underlain by a series of sandstones, shales, and coals that were deposited in brackish and marine environments during the Pennsylvanian Period (Williams 1960). These strata compose (from oldest to youngest) the Connoquenessing, Mercer, and Homewood Formations of the lower and middle Pennsylvanian Pottsville Group; and the Clarion and Kittanning Formations of the middle and upper Pennsylvanian Allegheny Group (Berg et al. 1980, 1983; Buckwalter et al. 1981). A geologic section (see figure 2) was constructed from driller's logs of the rocks encountered during installation of monitoring wells. Fine-grained, white-to-gray sandstone is the predominant overburden lithology, and gray, interbedded shale and siltstone lie above and below the coals. Limestone is sparse to absent in the study area. Bedrock dips approximately 0.5 to 1.0 degree to the northwest.

Mineralogy was determined by x-ray diffraction analysis of crushed rock samples from a 170-ft-long drill core through bedrock from the base of the lower Kittanning coal into the upper part of the Connoquenessing sandstone (well 14 in figure 2). The predominant minerals are aluminosilicates (see table 1): Quartz and kaolinite are present in every horizon; microcline, muscovite, illite, and chlorite are present in most non-coal horizons. Calcite is present only as a trace mineral in the deep shale and siltstone bedrock, and siderite is present in the siltstone and shale horizons above and below the Clarion and Mercer coals. Pyrite and marcasite are present primarily in the coal and secondarily in the shale samples. The ferric sulfates roemerite, copiapite, coquimbite, and jarosite are present, concentrated within several-inch-thick layers in the upper and lower Clarion coals and as trace minerals in the Mercer coals. The sulfate minerals occur as white and yellow efflorescences in cleats and on the surface of the coal samples. Much of the oxidation of pyrite to produce the sulfate minerals probably occurred in situ, prior to core collection, because the Clarion coals in the highwall were dewatered and aerated during mining when the water table was

lowered about 25 ft to a level at, or below, the altitude of the base of the lower Clarion coal (see figure 2). However, some ferric sulfates, especially in deeper samples in the Homewood and Mercer Formations also could have formed while the core was in storage. Goethite, the only iron oxide identified, was found in one sandstone sample collected above the upper Clarion coal. Hematite, melanterite, gypsum, dolomite, and pyrolusite were not identified in any samples. The sulfur minerals and calcite are sparse and occur in discrete layers--thus their presence is difficult to confirm by x-ray analysis of composite samples--however, these phases are relatively reactive and are likely to control the quality of ground water.

Chemical analysis of the pulverized rock samples from the drill core (well 14 in figure 2) was performed to confirm and quantify the presence of carbonate, sulfate, and sulfide minerals. The samples were analyzed for neutralization potential (NP), pH of a 1:1 water:rock paste, and concentrations of total sulfur, forms of sulfur (Sobek et al. 1978; Noll et al. 1988), iron, and manganese (see table 2). None of the samples effervesced upon addition of dilute hydrochloric acid (HCl), nor did any have substantial NP (expressed as ppt = tons $CaCO_3$ per thousand tons). The highest NP value is 47.4 ppt for a composite sample from a 0.5-ft-thick horizon, which did not contain detectible calcite. Because the samples did not react visibly with HCl, NP values greater than 30 ppt probably indicate the presence of siderite rather than calcite or dolomite (Brady and Hornberger 1989; Morrison et al. 1990a). The rock samples containing detectible siderite (see tables 1 and 2) have NP values ranging from 1.3 to 47.4 ppt. Negative values of NP indicate production of acid, corresponding with low values of paste pH (less than 4). The rock samples containing iron-sulfide and -sulfate minerals have NP values ranging from -134.9 to -0.3 ppt.

On the basis of the concentration of total sulfur-- which consists of sulfide, sulfate, and organic sulfur, generally in order of decreasing abundance--and molar ratios of inorganic sulfur to iron (Sin/Fe) (see table 2), two groups of samples can be distinguished: (1) high-sulfur coal samples containing greater than 2% total sulfur and having Sin/Fe values of 1.2 to 2.1, and (2) low-sulfur, noncoal samples containing less than 0.61% total sulfur and having Sin/Fe values of less than 0.3. Of the high-sulfur group, the Clarion coals and the uppermost Mercer coal are at least 2 ft thick (respective depth intervals: 108.6-111.0; 123.2-126.8; 173.0-175.0), and contain 3.5% to 17% sulfur and 2% to 20% iron. The Sin/Fe values in the original,

TABLE 1.--Minerals identified in drill-core rock samples[1] by x-ray diffraction [● major; O minor; - not detected]

DEPTH INTERVAL[1]	GEO-LOGIC UNIT[2]	LITH-OLOGY[3]	QUARTZ & KAOLINITE	MUSCOVITE & ILLITE	MICROCLINE FELDSPAR	CHLORITE	CALCITE	SIDERITE	PYRITE MARCASITE	ROEMERITE COQUIMBITE COPIAPITE JAROSITE[4]	GOETHITE
46.8- 48.5	KTFM	CL	●	●	●	●	-	-	-	-	-
49.0- 50.0	KTFM	SH	●	●	●	-	-	●	-	-	-
58.0- 60.0	KTFM	ST	●	●	●	-	-	-	-	-	-
66.0- 66.5	VNFM	SS+LS	●	●	●	-	-	●	-	-	-
78.0- 80.0	CLFM	SS	●	●	-	●	-	-	-	-	-
82.0- 84.0	CLFM	SS	●	●	●	●	-	-	-	-	-
90.0- 92.0	CLFM	SS	●	●	●	●	-	●	-	-	-
102.0-104.0	CLFM	SS	●	●	●	●	-	-	-	-	●
108.6-108.9	CLUC	WH	●	-	-	-	-	-	●	●	-
109.5-111.0	CLUC	CO+WH	●	-	-	-	-	-	●	O	-
114.0-116.0	CLFM	SH+SS	●	●	●	O	-	●	-	-	-
123.2-123.4	CLLC	CO+WH	●	●	●	●	-	-	-	O	-
125.5-126.8	CLLC	CO+CL	●	-	-	-	-	-	●	●	-
129.8-131.8	HWFM	CL	●	●	●	-	-	-	-	-	-
137.7-139.0	HWFM	SH	●	-	O	-	-	-	O	-	-
143.5-144.2	HWFM	ST+SH	●	●	-	-	-	O	-	-	-
145.0-147.0	HWFM	ST	●	●	●	-	-	●	-	-	-
153.0-155.0	HWFM	ST	●	●	●	●	-	●	-	-	-
165.0-169.0	HWFM	ST	●	●	●	●	-	●	-	-	-
173.0-175.0	MRFM	CO+WH	●	●	-	●	-	-	●	O	-
175.3-178.0	MRFM	CL	●	●	-	●	O	●	-	-	-
181.9-182.6	MRFM	SH+CO	●	●	O	-	-	-	●	-	-
184.0-185.0	MRFM	CL	●	●	●	-	-	O	-	-	-
188.5-189.0	MRFM	CO	●	●	-	O	-	-	●	O	-
189.5-191.5	MRFM	SH+ST	●	●	●	●	-	-	-	-	-
196.5-199.5	CQFM	SS+ST	●	●	●	●	O	-	-	-	-

[1]Drill core from well 14 location (fig. 2). Composite sample depth interval, in feet below present land surface. The following depth ranges indicate the equivalent position of screened intervals for monitor wells: 0-48 ft = well 14C; 60-127 ft = wells 14B and 15B; 132-195 ft = wells 14A, 15A, and 17A; 197-215 ft = wells 14, 15, and 17.

[2]Geologic units correspond to those in geologic section (fig. 2): KTFM = Kittanning Formation; VNFM = Vanport Formation; CLFM = Clarion Formation; CLUC = upper Clarion coal; CLLC = lower Clarion coal; HWFM = Homewood Formation; MRFM = Mercer Formation; CQFM = Connoquenessing Formation.

[3]Lithology determined by hand-specimen analysis: SS = sandstone; ST = siltstone; SH = shale; CL = underclay; WH = white efflorescence; CO = coal; LS = limestone.

[4]Stoichiometric formulas for ferro-ferric-sulfate minerals are indicated in table 2.

TABLE 2.--Rock sample depth, thickness, neutralization potential (NP), chemical concentrations and ratios

[no data (-); depth in feet below surface (ft); thickness in feet (ft);
weight percent (%) or parts per thousand (ppt); molar ratio (M/M)]

DEPTH INTERVAL[1] (ft)	THICK-NESS (ft)	GEO-LOGIC UNIT[2]	LITH-OLOGY[3]	PASTE pH	NP (ppt)	SULFUR, TOTAL (%)	SUL-FIDE (%)	SUL-FATE (%)	SUL-FUR, ORGN[4] (%)	MANG-ANESE (%)	IRON, TOTAL (%)	S/Fe[4] (M/M)	Sin/Fe[4] (M/M)	Mn/Fe (M/M)
46.8- 48.5	1.7	KTFM	CL	4.4	2.68	0.42	-	-	-	0.047	4.11	0.178	-	0.012
49.0- 50.0	1.0	KTFM	SH	5.2	1.32	.02	0.02	<0.01	<0.01	.007	1.16	.030	0.015	.006
58.0- 60.0	2.0	KTFM	ST	5.7	1.99	.00	-	-	-	.109	9.95	.000	-	.011
66.0- 66.5	.5	VNFM	SS+LS	7.2	47.36	.00	-	-	-	.307	20.40	.000	-	.015
78.0- 80.0	2.0	CLFM	SS	7.0	3.99	.00	-	-	-	.018	1.33	.000	-	.013
82.0- 84.0	2.0	CLFM	SS	7.4	5.88	.00	-	-	-	.022	1.57	.000	-	.014
90.0- 92.0	2.0	CLFM	SS	7.0	6.15	.01	-	-	-	.018	1.45	.012	-	.013
102.0-104.0	2.0	CLFM	SS	6.2	5.49	.06	-	-	-	.026	1.24	.084	-	.021
108.6-108.9	.3	CLUC	WH	1.2	-134.94	17.40	10.61	5.71	1.08	.021	20.32	1.492	1.399	.001
109.5-111.0	1.5	CLUC	CO+WH	2.8	-8.27	3.48	1.88	.27	1.33	.001	1.78	3.413	2.109	.001
114.0-116.0	2.0	CLFM	SH+SS	4.0	5.36	.83	-	-	-	.030	4.65	.311	-	.007
123.2-123.4	.2	CLLC	CO+WH	2.5	-25.44	5.54	4.33	1.11	.10	.075	7.17	1.346	1.322	.011
125.5-126.8	1.3	CLLC	CO+CL	2.4	-27.76	4.35	3.07	1.01	.27	.013	4.51	1.679	1.575	.003
129.8-131.8	2.0	HWFM	CL	6.1	2.08	.11	-	-	-	.004	1.18	.162	-	.004
137.7-139.0	1.3	HWFM	SH	4.2	5.00	.61	.43	.11	.07	.043	3.47	.307	.272	.013
143.5-144.2	.7	HWFM	ST+SH	5.7	15.91	.24	.16	.05	.03	.032	3.97	.105	.092	.008
145.0-147.0	2.0	HWFM	ST	7.3	16.19	.03	-	-	-	.029	3.18	.016	-	.009
153.0-155.0	2.0	HWFM	ST	7.4	45.55	.20	-	-	-	.100	5.64	.062	-	.018
165.0-169.0	4.0	HWFM	ST	6.8	13.06	.17	.12	.02	.03	.077	4.95	.060	.049	.016
173.0-175.0	2.0	MRFM	CO+WH	3.5	-.32	3.44	2.97	.26	.21	.033	4.50	1.332	1.250	.007
175.3-178.0	2.7	MRFM	CL	4.0	-.11	.39	-	-	-	.025	3.11	.218	-	.008
181.9-182.6	.7	MRFM	SH+CO	3.4	-3.48	2.15	1.50	.13	.52	.002	1.64	2.281	1.730	.001
184.0-185.0	1.0	MRFM	CL	7.0	1.00	.12	-	-	-	.005	1.07	.195	-	.005
188.5-189.0	.5	MRFM	CO	2.3	-10.99	4.11	3.13	.49	.49	.009	4.57	1.565	1.379	.002
189.5-191.5	2.0	MRFM	SH+ST	4.3	-.06	.31	-	-	-	.010	1.73	.312	-	.006
196.5-199.5	3.0	CQFM	SS+ST	5.6	.36	.17	-	-	-	.011	1.35	.219	-	.008

[1] Drill core from well 14 location (fig. 2). Composite sample depth interval, in feet below present land surface.

[2] Geologic units correspond to those in geologic section (fig. 2): KTFM = Kittanning Formation; VNFM = Vanport Formation; CLFM = Clarion Formation; CLUC = upper Clarion coal; CLLC = lower Clarion coal; HWFM = Homewood Formation; MRFM = Mercer Formation; CQFM = Connoquenessing Formation.

[3] Lithology determined by hand-specimen analysis: SS = sandstone; ST = siltstone; SH = shale; CL = underclay; WH = white efflorescence; CO = coal; LS = limestone.

[4] Molar ratios of total sulfur to iron (S/Fe) for rock samples include organic sulfur. Fe/S values for the minerals below can be compared with the ratio of inorganic sulfur to iron (Sin/Fe).

pyrite	FeS_2	S/Fe = 2.00	marcasite	FeS_2	S/Fe = 2.00
roemerite	$Fe^{2+}Fe_2^{3+}(SO_4)_4 \cdot 14H_2O$	S/Fe = 1.33	copiapite	$Fe^{2+}Fe_4^{3+}(SO_4)_6 \cdot 20H_2O(OH)_2$	S/Fe = 1.20
coquimbite	$Fe_2(SO_4)_3 \cdot 9H_2O$	S/Fe = 1.50	jarosite	$KFe_3(SO_4)_2(OH)_6$	S/Fe = 0.66

Page 50

unweathered minerals are unknown; however, values of 1.2 to 2.1 for the coal samples imply the presence iron-sulfide and weathered iron-hydroxide and -sulfate minerals, which have Sin/Fe from 0.66 to 2.0 (see table 2, footnote 3). The ferric-sulfate minerals roemerite, copiapite, coquimbite, and jarosite have Sin/Fe values of less than 2.0. If all iron and sulfur in the unweathered coal samples were in the form of pyrite (+ marcasite), the Sin/Fe ratio would equal 2.0; however, Sin/Fe values substantially less than 2.0 would indicate weathering (oxidation and leaching) because iron generally is less mobile than sulfate. Oxidation of pyrite under unsaturated, nonrecharge (humid air) conditions would conserve the ratio of Sin/Fe = 2.0, which would be expected if the oxidation of pyrite took place while the samples aged in core boxes before analysis. Oxidation of organic forms of sulfur would increase the Sin/Fe ratio. As for low-sulfur, noncoal samples, a combination of pyrite, goethite, siderite, and (or) chlorite will yield Sin/Fe values less than 0.3.

The rock-core chemical data in table 2 also indicate sources of Mn, a major cation in AMD. Manganese is present in all the rock samples, and ranges in concentration from about 0.001% to 0.3%. No dominantly Mn-bearing minerals were identified by x-ray diffraction, which indicates that minerals such as manganite ($MnOOH$) or pyrolusite (MnO_2) which commonly form coatings within joints and fractures, are not abundant. Manganese is likely to occur in silicate minerals, such as chlorite, which is abundant throughout the section. Although pyrite normally contains trace quantities of Mn (Gang and Langmuir 1974) the coal samples containing detectable pyrite and (or) iron-sulfate minerals have a low molar ratio of manganese to iron (Mn/Fe), ranging from 0.001 to 0.007, which suggests that neither coal nor pyrite is a major source of Mn. However, the higher Mn concentrations (greater than 0.04%) occur in samples containing relatively high Fe, and having a relatively high Mn/Fe, ranging from about 0.01 to 0.02. Most, but not all, the high-Mn samples contain detectable siderite (see tables 1 and 2). Manganese commonly occurs as a trace impurity in siderite, which tends to weather producing iron-manganese oxyhydroxide minerals (Senkayi et al. 1986). The samples containing siderite have Mn/Fe ratios ranging from 0.006 to 0.018, which are consistent with a ratio of 0.012 for a siderite stoichiometry of $(Fe_{0.86}Mn_{0.01}Mg_{0.02}Ca_{0.1})CO_3$, reported by Morrison et al. (1990b).

Ground-Water Hydrology

Three monitoring well nests were installed by the mine operator in a line roughly parallel to the east-to-west direction of ground-water flow (see figures 1 and 2): Nest 14 is in the untreated zone, nest 15 is in the sludge-covered zone, and nest 17 is below the toe of spoil. Nest 14 consists of 4 wells (14, 14A, 14B, 14C), nest 15 consists of 3 wells (15, 15A, 15B), and nest 17 consists of 2 wells (17, 17A). Each well was constructed of 2-in diameter polyvinyl-chloride (PVC) pipe installed in separate drill holes. The annulus above the screen was filled with grout and that below the screen with rock cuttings. Wells 14, 15, and 17 were screened in the Connoquenessing Formation sandstone. Wells 14A, 15A, and 17A were screened in the overlying Mercer Formation coal and shale. Wells 14B and 15B were completed in the lower Clarion coal horizon; well 14B was screened through bedrock and well 15B was screened through sludge-covered mine spoil. Well 14C was screened through the untreated mine spoil at the Kittanning coal horizon on the upper bench.

Static-water levels in the wells were measured monthly from June 1986 through November 1989. The mine spoil on the upper bench forms a perched aquifer with a saturated thickness that has fluctuated seasonally from 6 to 9 ft. However, the mine spoil on the lower bench is part of the water-table aquifer, which is continuous across the site (see figures 1 and 3). The saturated thickness of the mine spoil on the lower bench has fluctuated from about 10 to 21 ft during the period of study. The water table within the adjacent unmined zone (highwall) has fluctuated less than 7 ft, and has remained at least 10 ft above the upper Clarion coal during the post-reclamation period of study. However, during recent mining, the water table probably was lowered to a level about 25 ft below its present location. Such transient hydrologic conditions are ideal for weathering pyrite and forming Fe^{3+} and SO_4^{2-} in the mine spoil (current formation) and unmined coal in the highwall (past formation).

A crude analytical water budget for the period of study includes measured seepage discharge rates and an estimated annual recharge of 45 percent of the cumulative annual precipitation of 43 in. Rainfall data were obtained from records of a National Oceanic and Atmospheric Administration (NOAA) weather station at Clarion about 4 mi northeast of the study area (NOAA 1987, 1988). The recharge rate of 45 percent of precipitation (45 % P) assumes 52 % P is lost by evapotranspiration, which is consistent with that for a nearby mine site (Henke 1985), and only 3 % P is lost as runoff because sedimentation ponds prevent most runoff

Page 51

EXPLANATION

—⟵— Flow line, arrow indicates direction

Hydraulic conductivity

K1 10,000 ft/yr
K2 2,700 ft/yr
K3 1,100 ft/yr
K4 700 ft/yr
K5 510 ft/yr
K6 400 ft/yr
K7 2.4 ft/yr
K8 2.1 ft/yr
K9 1.1 ft/yr

WELL NEST 17
17 17A

WELL NEST 15
15 15A 15B

WELL NEST 14
14 14A 14B 14C

perched water table

saturated water table

water table

Stream

K1

K2

K5
K3
K8
K7
K3
K8
K7
K4
K9
K6

VERTICAL EXAGERATION X4

Figure 3.--Ground-water table and flow directions along an east-west section through the mine (Saad and Cravotta, 1991). Model boundaries include: top, constant flux; east, west, and bottom, no flow.

from leaving the mine site. Although the average recharge is 45 % P, the recharge rate to different zones is expected to vary depending on the distribution of mine spoil and occurrence of aquitards (perched aquifer) and seepage areas (toe of spoil).

Geologic and hydrologic data were used to construct a two-dimensional, cross-sectional, layered model of ground-water flow through the mine spoil and underlying bedrock (see figure 3) (Saad and Cravotta 1991). Modeling was conducted using the steady-state option of the finite-difference computer program, MODFLOW (McDonald and Harbaugh 1988) and by simulating a range of boundary conditions and probable hydraulic conductivities. The eastern and western divides and

base of the flow system were simulated as no-flow boundaries, and the saturated water table was simulated as a constant-recharge boundary. Different recharge rates were assumed for zones corresponding to the upper bench (below the perched aquifer), lower bench, and toe of spoil to the stream (see figure 3). Seventy-five percent of the recharge to the perched aquifer was assumed to percolate to the underlying saturated bedrock (34 % P), and the remainder was assumed to flow to the highwall and to percolate, in addition to rainfall recharge (45 % P), through mine spoil of the lower bench. Similarly, seepage water from the toe of spoil on the lower bench was added to rainfall recharging the water table between the toe of spoil and the stream. Hydraulic conductivities were varied to reflect three

different hydrogeologic units—spoil, coal and sandstone, and shale and underclay—and were adjusted to match the median static-water levels measured in seven of the nine wells along the cross section. The water levels in wells 14 and 14A were not used because the well casing above the screened intervals is known to leak. The resultant ground-water heads and flow paths were computed and plotted by use the computer programs, CONTOUR (Harbaugh 1990) and MOOPATH (Pollack 1989), respectively.

In general, directions of ground-water flow are dominantly horizontal near the water table in the coal and mine spoil, downward through underlying zones across most of the section, and both downward and westward through the deeper underlying bedrock (see figure 3). However, near the stream-discharge zone at the western boundary, ground-water flow is directed upward to the streambed. Flow paths are predominantly horizontal through transmissive units (spoil, coal, and sandstone) and vertical through confining units (shale and underclay). The flow paths through screened intervals of upflow and downflow wells are of particular interest because these define potential reaction paths for water-quality changes.

Conceptual Model of Oxygen Transport

The concept of water-unsaturated, oxygenated zones (open system) versus water-saturated, oxygen-limited zones (closed system) (see figure 4) provides a basis for evaluating where and to what extent oxidation reactions may occur in the subsurface (Champ et al. 1979). The transport of O_2 into unsaturated mine spoil
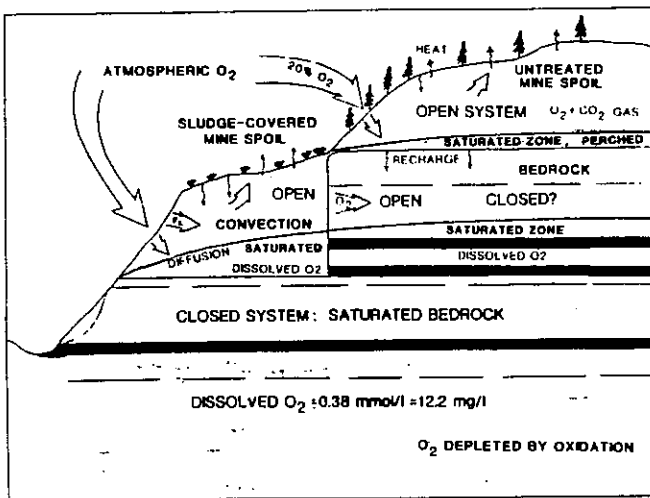
Figure 4.—Conceptual model of oxygen transport into subsurface water-unsaturated and -saturated zones of the mine.

is likely to be driven by thermal convection (Cathles 1982), diffusion (Jaynes et al. 1984a,b), and (or) displacement by recharge waters, depending on unsaturated zone temperature, permeability, pore-gas composition, and moisture conditions. Pyrite oxidation depletes O_2 and warms air within the unsaturated mine spoil. Temperature and gas profiles were not measured in the vadose zone; however, diffusion to O_2-depleted zones will occur, and if the temperature gradients and permeability are large, as expected, convection will predominate as the warm air to rises through the spoil to the surface. In exchange, fresh oxygenated air from the atmosphere flows through the steep, barren slopes into the unsaturated spoil and fractured bedrock. Moisture in the fresh air can condense on mineral surfaces. Thus, water and abundant O_2 are available in the vadose zone (open system) to react with pyrite producing ferric-hydroxide and -sulfate minerals (reactions 4 and 5). Below the water table, however, transport of O_2 is limited by its solubility and time required for diffusion in ground water. Thus, the extent to which oxygenation reactions (such as 1 through 5) occur will be limited by the concentration of DO (closed system). For example, ground water at $6^{\circ}C$ can attain a maximum equilibrium concentration of DO of 0.38 millimole per liter (mmol/1) or 12.2 milligrams per liter (mg/1) (Orever 1982, p. 287). As this oxygen-saturated water flows downward from the water table to deeper zones, the oxidation of organic matter, iron, manganese, sulfur, and other reduced elements will deplete DO and produce anoxic conditions at some point along the flow path. Thus, if pyrite oxidation occurs in a closed system by reaction 1, where 1 mol of FeS_2 reacts with 3.5 mol of O_2 producing 2 mol of SO_4^{2-}, then reaction with 0.38 mmol/1 of O_2 can produce only 0.22 mmol/1 of SO_4^{2-} (= 20.8 mg/1). In contrast, additional and potentially much greater quantities of SO_4^{2-} may be produced in the absence of DO if pyrite oxidation occurs by reactions 6 or 8. However, those reactions still depend on the previous production of Fe^{3+} by reaction 2, which involves O_2.

Geochemical Evolution of Acidic Ground Water

An examination of the geologic and hydrologic data presented in the previous sections shows that certain minerals appear consistently in the rocks of the overburden, coal, underburden, and mine spoil (see table 1), and that the ground water tends to flow from oxic zones near the water table to deeper potentially anoxic zones. The objective of this section is to describe the hydrochemical trends along potential flow paths and to evaluate the formation of acidic ground water by reactions between gaseous, aqueous, and solid phases in systems that are open or closed with respect to O_2.

Hydrochemical Trends

Water-quality data were collected quarterly in December 1986 through September 1989 to characterize hydrochemical trends as affected by surface coal mining and reclamation with sewage sludge. Field measurements and water-quality sampling were conducted after purging stagnant water from wells with PVC bailers. Measurements of pH, DO, platinum-electrode potential (Eh), specific conductance, and temperature were conducted following methods of Wood (1976). DO and temperature were determined by suspending electrometric probes downhole, and specific conductance, pH, and Eh were determined at the well head. Samples for analysis of cations (Fe, Mn, Al, Mg, Ca, Na, K, Si, Ba, Cd, Cu, Ni, Pb, Sr, Zn) were filtered through 0.45-micrometer porosity filters, transferred to acid-rinsed polyethylene bottles, and preserved with nitric acid. Samples for analysis of Fe^{2+} were not filtered, were stored in polyethylene bottles, and preserved with sulfuric acid. Samples for analysis of anions (SO_4, Cl), nutrients (PO_4-P, NO_3-N, NH_4-N), acidity, and alkalinity were not filtered and were stored in polyethylene bottles on ice until analyzed. The water samples were analyzed at the PaDER Bureau of Laboratories facility in Harrisburg, Pa., following methods mainly of Skougstad et al. (1979). Concentrations of cations and silica were determined by inductively coupled plasma emission (ICPE) or atomic absorption (AA) spectrometry; alkalinity and acidity were determined by titration; sulfate was measured by turbidimetry; ferrous iron, phosphorus, nitrogen, and chloride were measured by colorimetry.

Hydrochemical trends, which are apparent as changes in DO, Eh, pH, and solute concentrations (see figure 5), result from interacting physical, biochemical, and geochemical processes. Important physical processes include gas movement, ground-water flow (solute transport), dispersion, dilution, filtration, and evaporation. Biochemical processes include reaction catalysis (iron and sulfur oxidation), cell synthesis (uptake of CO_2 and nutrients), respiration and decay (uptake of O_2 and release of CO_2 and nutrients), and transpiration. Major geochemical processes include ion-complexation, acid-base, oxidation-reduction, precipitation-dissolution, and sorption (ion-exchange) reactions. Modeling to account for hydrochemical variations attempts to relate many of these interacting factors and emphasizes the geochemical interactions between the ground water and solid aquifer matrix.

Most minerals that compose the overburden, coal, and underburden are probable reactants under acid conditions, and minerals that precipitate at seepage zones indicate possible products. To test the thermodynamic potential for dissolution or precipitation of mineral phases, equilibrium speciation and mineral saturation indices were computed using WATEQ4F (Ball et al. 1987). The saturation index (SI) is defined as:

$$SI = \log (IAP/K_T), \qquad (14)$$

where IAP is the measured ion activity product for a solid in water, and K_T is the thermodynamic equilibrium constant for the same solid in the water, at the temperature of interest (Drever 1982; Plummer et al. 1990). If SI is zero, the water is in equilibrium with respect to the mineral. If SI is negative, the water is undersaturated with respect to the mineral and could dissolve it (reactants). If SI is positive, the water is supersaturated and could not dissolve the mineral, but could potentially precipitate it (products). The complete hydrochemical data for the quarterly samples from wells in nests 14 and 15 which were used to calculate median values and corresponding saturation indices are contained in the USGS Quality of Water (QWDATA) data base. The data and SI results judged to be useful in the geochemical mass-transfer models are presented in figures 5 and 6, respectively.

Most mineral phases are not in equilibrium with the ground water; however, SIs for gypsum, $AlOHSO_4$, and amorphous silica are near zero (∓ 0.5) for most water samples (see figure 6). The waters from all wells are supersaturated with respect to chalcedony (cryptocrystalline silica), quartz, jarosite, and goethite. Slight oversaturation of waters with respect to chalcedony and equilibrium with amorphous silica is expected where silicate minerals react in an acidic system. Supersaturation with respect to jarosite and goethite implies that Fe and S are not precipitated as fast as they are produced by the oxidation of pyrite and dissolution of hydrated ferric-sulfate minerals. Kinetic factors favor the precipitation of ferrihydrite instead of goethite or jarosite (Whittemore and Langmuir 1975; Nordstrom et al. 1979); waters from wells 14, 14A, 14B, and 14C are oversaturated and those from wells 15, 15A, and 15B are undersaturated with respect to ferrihydrite. All samples also are undersaturated with respect to calcite, dolomite, siderite, gypsum, epsomite, barite, celestite, melanterite, and many aluminosilicates, most of which are not shown in figure 6. No thermodynamic data are available for roemerite, copiapite, or coquimbite, so that SI values for these minerals could not be calculated; however, a ferric-sulfate phase $Fe_2(SO_4)_3$ included in the WATEQ4F data base is consistently undersaturated (SI < -22). Potential solubility control of iron by ferrihydrite, goethite, and possibly jarosite(?) is consistent with
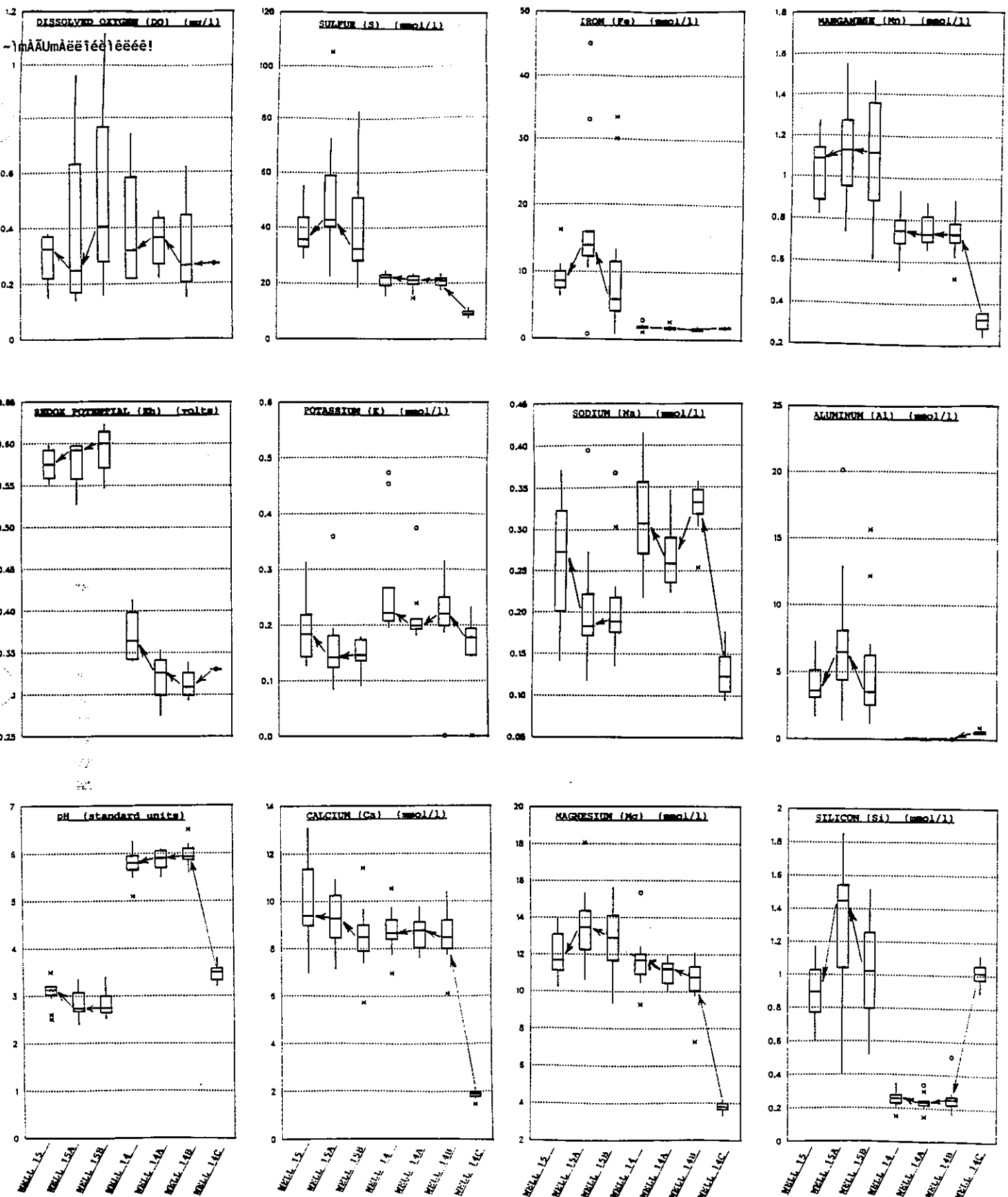
Figure 5.--Boxplots of DO, Eh, pH, and concentrations of major dissolved solutes in waters from well nests 14 and 15. Arrows indicate potential downward flow. Boxes are defined by the interquartile range (IQR = 25th to 75th percentiles). The median (50th percentile) is shown as a horizontal line within the box. Vertical lines are drawn to the data points farthest from the box, yet within a distance 1.5 times the IQR beyond the box. Extreme values beyond this distance are plotted individually (*, o).

results of work by Nordstrom et al. (1979) and Karathansis et al. (1988, 1990).

Figure 5 shows boxplots of the major water-quality data used for equilibrium speciation (mineral SI) and mass-balance calculations. Data for DO, Eh, pH, and major solutes are indicated for samples from well nest 14 beneath untreated spoil (wells 14C, 14B, 14A, and 14) and for samples from well nest 15 beneath sludge-treated spoil (wells 15B, 15A, and 15). Westward ground-water flow from well nest 14 to 15 is indicated in figure 3, which shows that within a given well nest, there also is potential for downward flow. Arrows drawn between medians in the boxes (see figure 5) indicate the downward flow potential within each well nest--wells 14C to 14B to 14A to 14 and wells 15B to 15A to 15. Dissolved SO_4^{2-} (shown as S) is useful as a reaction progress variable, because it is likely that the sulfide and sulfate minerals dissolve irreversibly in most of the system.

The waters from nest 14, generally contain negligible concentrations of DO (< 0.5 mg/1), which are relatively unchanged with depth (see figure 5); however, pH and concentrations of S, Mn, Ca, Mg, Na, and K increase downflow from the untreated mine spoil (well 14C) to underlying bedrock (well 14B). Waters from the bedrock (wells 14B, 14A, and 14) have similar quality. These trends suggest that acid produced in the mine spoil and shallow bedrock is neutralized by reaction with silicate and carbonate minerals in the bedrock. Concentrations of Fe appear to remain level and to be limited to some maximum, probably because of solubility control by precipitation of ferrihydrite or jarosite(?). Concentrations of Si and Al decrease downflow suggesting control by kaolinite and (or) gibbsite.

The waters from nest 15 also contain negligible DO, but relative to equivalent horizons in nest 14 (see figure 2), they have lower pH (< 3), higher Eh (> .5 volts), and generally greater concentrations of major ions (see figure 5). As in nest 14, the ground-water in bedrock beneath the mine spoil is more mineralized than the upflow water; however, the concentrations of S, Fe, Mn, Mg, Al, and Si rise and then fall with increasing depth from wells 15B to 15A to 15. The intermediate depth well 15A has the maximum concentrations of Fe, S, and Al, which may result from acid-generating reactions and partial neutralization by silicates. These waters also exhibit a relative depression in concentration of Na and K. A partial explanation for declines in Na and K downflow from wells 15B to 15A and in S and Fe downflow from wells 15A to 15 is that jarosite could be precipitating at depth. However, considering the data

for wells 15A and 15, the ratio of moles of S and Fe presumably lost from solution is greater than that expected considering the stoichiometry of jarosite, and there are corresponding lower concentrations of other solutes including Mg, Mn, Si, and Al in waters from well 15 relative to those from well 15A. These trends suggest the possibility of dilution by mixing of waters from above with less mineralized waters from the west.

Reaction-Path Modeling

The purpose of reaction-path modeling is (1) to explain the spatial hydrochemical changes, (2) to suggest the major reactant and product phases, and (3) to determine the variation in the quantity of each phase entering or leaving the ground-water system. The equations and principles of reaction-path modeling are given elsewhere (Plummer and Back 1980; Parkhurst et al. 1982; Plummer et al. 1983, 1990). Such modeling uses available hydrochemical data and attempts to find a set of mass-transfer reactions that are thermodynamically feasible and satisfy mass-and-electron balance criteria. Mass transfer is indicated

Initial Solution + Reactant Phases
      - Product Phases --> Final Solution.   (15)

In reaction 15, the initial and final solutions are the molal compositions of water samples from relative upflow and downflow points along a flow path, and the reactant and product phases are minerals and (or) gases that can feasibly react to produce or remove elements and balance electrons. A more complex equation involves the additional mixing of two initial solutions

Initial Solution 1 + Initial Solution 2
      + Reactant Phases - Product Phases -->
                        Final Solution.   (16)

The deeper wells in this study, for example well 15, are likely to sample water that has resulted from mixing of upflow waters as illustrated by the flow paths in figure 3 and water-quality data (see figure 5).

A mass-balance model must contain equal numbers of elements and phases, and for each element in the model, there must be at least one reactant or product phase containing the element. In the special case of a mixing model, one phase is excluded and the proportion of initial waters mixed is included to account for changes in one or more elements. For each chemical element included in the model, a linear mass-balance equation can be written that is the mass-difference between the initial and final solutions plus balancing quantities of reactant and product phases (minerals and gases)
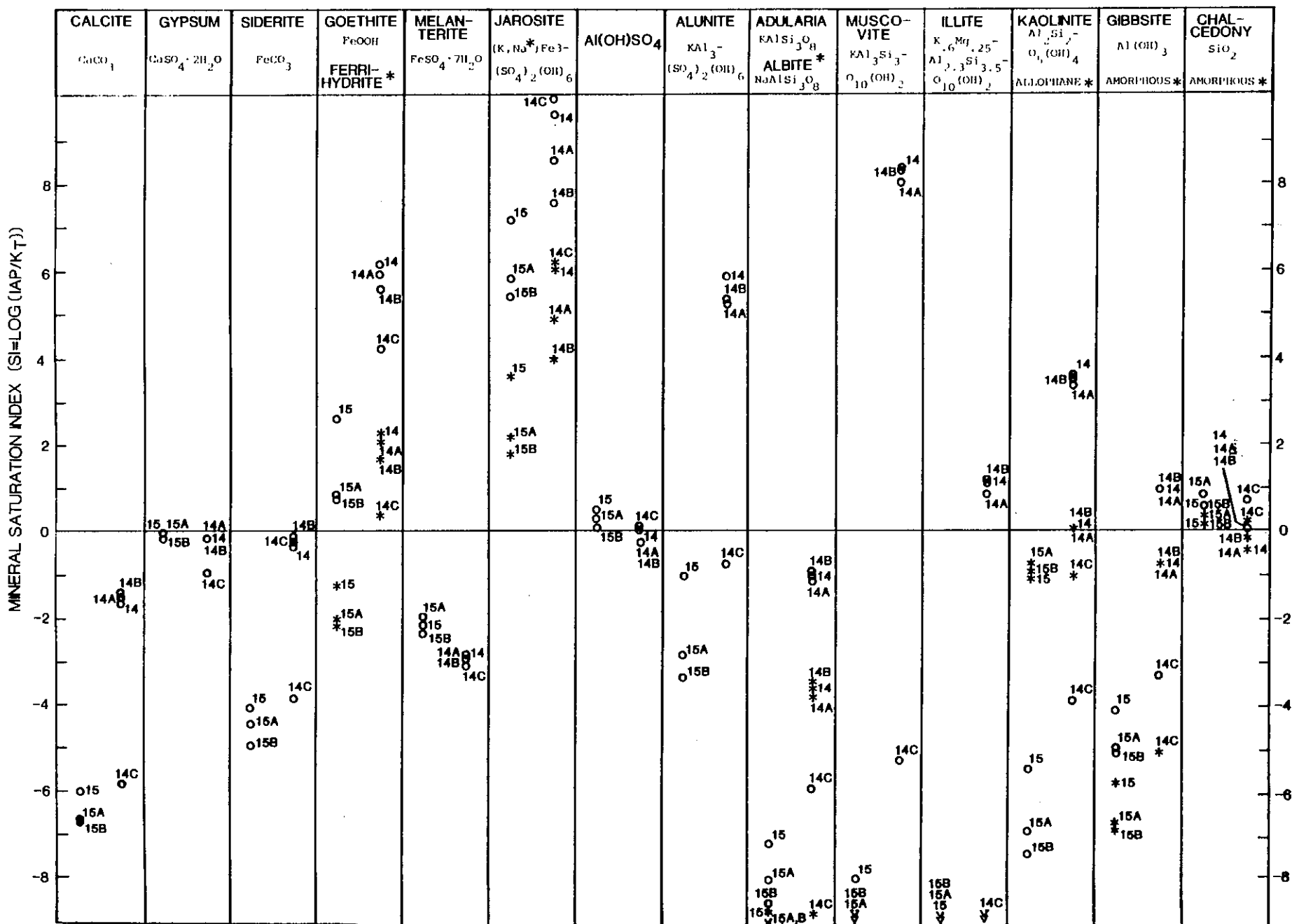
Figure 6.--Mineral saturation indices for median chemical concentrations, pH, Eh, DO, and temperature in ground-water samples. '*' indicates metastable, or less stable, phase relative to 'o'.

containing the element. Stoichiometric coefficients account for the number of moles of the element in the phases and the number of transferable electrons for redox-active species. The quantity of electrons transferred during mass-transfer reactions among the dissolved species and phases is computed by use of an operational "redox state" (RS) that is treated as an additional element (Parkhurst et al. 1982; Plummer et al. 1983, 1990). Thus, a reaction model is a particular choice of phases that react, or mix and react, to produce the measured final water composition.

Four different reaction-path scenarios (see figure 7) are presented to demonstrate the feasibility of pyrite oxidation in systems open and closed with respect to O_2 (see figure 4). The mass-balance models allow the evaluation of the amount of O_2 required to produce measured quantities of dissolved sulfate from pyrite and (or) ferro-ferric-sulfate minerals considering mineral and O_2 solubility constraints, as indicated by the mineral SI (see figure 6) and maximum DO (= 0.38 mmol/l) in a closed system. Additional constraints on "acceptable" models include the absolute change in major solute concentrations and the presence, or absence, of the phases along the flow path(s). The median molal concentrations of the elements and calculated RS for the water samples from nests 14 and 15 that are used as

Possible Reaction-Path Models:

14C --> 14B: Open system: Untreated spoil to underlying bedrock

14C + 14B --> 15B: Open system: Untreated spoil and unmined coal (highwall)
                                   to sludge-treated spoil

15B --> 15A: Closed system: Sludge-treated spoil to underlying bedrock

14 + 15A --> 15:   Closed system: Bedrock below untreated and sludge-treated
                                   areas to downflow bedrock

Figure 7.--Diagram showing a summary of potential flow paths for mixing and mass-transfer models. '▼' indicates median static water level.

input data in NEWBAL (Parkhurst et al. 1982) are summarized in table 3. In table 4, reactant minerals are shown with a "+" and product minerals with a "-" considering the SI calculated using the hydrochemical data. Results of the mass-balance calculations are summarized in table 5.

Open system: Downward flow from untreated spoil to underlying bedrock. A 70-ft difference in head between wells 14C and 14B suggests downward flow from the perched ground water in untreated mine spoil (well 14C) to the underlying bedrock aquifer (well 14B) (see figure 7). This system is probably open to O_2 along the flow path because intermediate zones are not saturated with water (see figures 3, 4). The downflow ground water contains greater concentrations of S and major cations except Fe, Si, and Al (see table 3 and figure 5) and is supersaturated with respect to ferrihydrite, jarosite, gibbsite, quartz, and kaolinite (see figure 6), which are potential product phases. Potential reactants include pyrite and roemerite, plus calcite, siderite, pyrolusite, and aluminosilicates to generate the remaining elevated cations. Pyrolusite contains Mn^{4+}, which may have a role similar to Fe^{3+}, in that both ions can oxidize sulfur.

Ten models were generated which satisfy mineral-solubility constraints and explain the changes in water chemistry from well 14C to 14B (see table 5). The major difference among the models is between pyrite or roemerite as the source of S and between siderite and pyrolusite as the source of Mn in solution. Model 5 involves reactions with pyrite, roemerite, and siderite, all of which are sources of Fe. The production of sulfate from pyrite (reaction 4) would require 26.7 to 84.9 mmol O_2; the latter is 223 times the maximum solubility of O_2. However, since the sulfur and most of the iron in roemerite is already oxidized, the same quantity of sulfate can be generated from roemerite with only 0.72 mmol O_2; that is 1.8 times the maximum solubility of O_2 (0.38 mmol/l). Because the system is open to O_2, any model is acceptable. Models 3 and 10 involve the least mass transfer: they react pyrite or roemerite plus pyrite, and pyrolusite, calcite, and aluminosilicate minerals (chlorite, illite, microcline), and produce ferrihydrite, jarosite, kaolinite, amorphous silica, and carbon dioxide (CO_2) gas.

Open system: Mixing of waters from untreated spoil and unmined coal to sludge-treated spoil. An 11-ft difference in head between wells 14B and 15B, screened through the intact and mined Clarion coal horizon, respectively (see figure 7), suggests that flow from the highwall, downdip to the mine spoil occurs. An 80-ft difference in head between wells 14C and 15B also
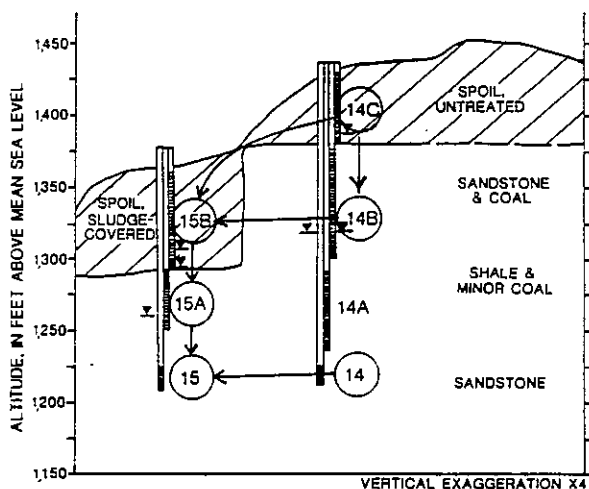
TABLE 3.--Median values of concentrations of major dissolved solutes and
operational redox state[1] (RS) in ground-water samples used in mass-balance
computations [units are mmol/kg]

ELEMENT	WELL 14	WELL 14A	WELL 14B	WELL 14C	WELL 15	WELL 15A	WELL 15B
Ca	8.658	8.770	8.471	1.901	9.406	9.294	8.483
Mg	11.333	11.251	10.777	3.747	11.682	13.472	12.896
Na	0.307	0.260	0.332	0.117	0.273	0.182	0.189
K	0.222	0.199	0.220	0.178	0.184	0.142	0.145
Cl	0.085	0.085	0.085	0.085	0.056	0.056	0.056
C	8.360	8.170	9.400	6.780	6.780	6.780	6.780
S	22.168	21.101	20.867	8.890	35.702	42.973	32.558
Fe	1.816	1.771	1.590	1.760	8.648	13.934	5.962
Mn	0.749	0.733	0.732	0.322	1.088	1.130	1.118
Si	0.259	0.235	0.254	1.015	0.896	1.449	1.024
Al	0.013	0.009	0.009	0.537	3.610	6.468	3.506
RS	171.805	164.355	167.330	84.593	258.612	311.356	229.589

[1]Redox state: RS = S*6 + C*4 + Fe(II)*2 + Fe(III)*3 + Mn*2.

TABLE 4.--Stoichiometry[1] reactivity[2] and operational redox state[3] (RS) of
potential reactant and product phases used in mass-balance computations
[units are mmol]

```
O2 GAS        +RS 4.00
PYRITE        +Fe 1.00   S  2.00   RS 0.00
ROEMERITE     +Fe 3.00   S  4.00   RS32.00
FERRIHYORITE   Fe 1.00   RS 3.00
NA-JAROSITE   -Na 1.00   Fe 3.00   S  2.00    RS21.00
K-JAROSITE    -K  1.00   Fe 3.00   S  2.00    RS21.00
PYROLUSITE    +Mn 1.00   RS 4.00
SIDERITE      +Fe 0.875  Mn 0.015  Mg 0.02   Ca 0.10   C  1.00   RS 5.78
CALCITE       +Ca 1.00   C  1.00   RS 4.00
CHLORITE      +Mg 5.00   Al 2.00   Si 3.00
ILLITE         K  0.60   Mg 0.25   Al 2.30   Si 3.50
MICROCLINE    +K  0.85   Na 0.15   Al 1.00   Si 3.00
KAOLINITE      Al 2.00   Si 2.00
SiO2          -Si 1.00
CO2 GAS       -C  1.00   RS 4.00
```

[1]Stoichiometry excludes hydrogen and oxygen (see Parkhurst and others, 1982).

[2]Reactivity defined by saturation index (SI, fig. 6): '+' indicates reactant
(SI < 0); '-' indicates product (SI > 0); no sign indicates SI could be
positive or negative depending on the particular sample.

[3]Redox state for minerals computed considering redox active components (S, C,
Fe, Mn, O) as defined by Parkhurst and others (1982).

suggests potential flow from the perched aquifer (well 14C). Because the water table defines this mixing flow path (see figure 3), the system is probably open with respect to O_2. The downflow water beneath sludge-treated spoil contains greater concentrations of S, Fe, Mn, Ca, Mg, Si, and Al, and intermediate concentrations of Na and K relative to the upflow sources (see table 3). Downflow waters are supersaturated with respect to amorphous silica, goethite, and jarosite (see figure 6). Jarosite may precipitate and thus account for downflow decreases in concentrations of Na and K. Reactions with pyrite, roemerite, and (or) siderite may produce the observed increases in S, Fe, and Mn. Neutralization reactions with calcite and aluminosilicate minerals such as chlorite, microcline, and kaolinite are probable sources of Al, Mg, Na, K, and Si.

Ten mixing models were generated which satisfy the constraints (see table 5). Although the mixing ratios are different, they all indicate a greater contribution of water from the perched aquifer (67 to 85 percent), which is consistent with the expectation of greater flow rates in mine spoil relative to unmined coal. Some models involve O_2 and some do not; however, all involve reaction with pyrolusite. Models 1, 3, 5, and 7 involve reactions with pyrite and 33 to 51 mmol of O_2. Models 2 and 8 involve equivalent reactions with roemerite and 7 to 10 mmol of O_2 to produce dissolved S and Fe plus ferrihydrite (or goethite) and minor jarosite. Models 4, 6, 9, and 10 do not involve O_2: Models 4 and 6 involve reactions with roemerite and pyrite (reaction 8), and models 9 and 10 involve reactions with roemerite and pyrolusite. Chlorite, calcite or siderite, and microcline or kaolinite, also are reacted in the models. Silica and CO_2 are produced. Because the system is open with respect to O_2 all ten models are acceptable. Models 5 and 6, which involve the least mass transfer, react pyrite or roemerite plus pyrite, and pyrolusite, calcite, chlorite, and kaolinite, and produce ferrihydrite, minor jarosite, silica, and CO_2.

Closed system: Downward flow from sludge-treated spoil to underlying bedrock. A 17-ft difference in head between wells 15B and 15A suggests potential downward flow from the sludge-treated mine spoil to underlying bedrock (see figure 7). The flow path is water saturated and probably closed to O_2. Relative to the water from well 15B, the final water at well 15A contains greater concentrations of S, Fe, Mn, Al, Ca, Mg, and Si, and approximately unchanged, but lesser concentrations of Na and K (see table 3). Reactions with pyrite, roemerite, and siderite can produce the observed increases in Fe and S. Jarosite, which is supersaturated in both upflow and downflow waters can precipitate providing a sink for K and Na.

Aluminosilicate minerals and calcite can dissolve producing Ca, Mg, Al, and Si.

Four mass-transfer models were generated which satisfied the input constraints (see table 5). The major difference among the models is if pyrite reacts with DO or if roemerite reacts without DO to produce increased iron and sulfate in the downflow solution. All four models include roemerite as a reactant. In model 1, 1 mmol of pyrite is oxidized by 3.5 mmol of O_2 (reaction 1), which is nearly 9 times the maximum O_2 solubility. However, in models 2, 3, and 4, roemerite and small quanitities of pyrite react under anoxic conditions. Model 1 does not meet the closed system criteria for acceptability ($O_2 \lesssim 0.38$); however, models 2, 3, and 4 do not involve O_2 and can occur in a system closed to O_2. Therefore, if previously formed ferric sulfate or ferric-ions are transported along the flow path, substantial quantities of sulfate can be generated under anoxic conditions, by the dissolution of "stored" ferric salts and by the oxidation of pyrite by Fe^{3+}.

Closed system: Mixing of waters from bedrock below untreated and sludge-treated areas to downflow bedrock. A 25-ft difference in head between wells 15A and 15 suggests a strong potential for downward flow from the bedrock beneath sludge-treated mine spoil (well 15A) to underlying bedrock (well 15), and a 43-ft difference in head between wells 15A and 14 suggests potential for lateral flow to well 15 (see figure 7). Both vertical and lateral flow paths are water saturated and probably closed to O_2. The water at well 15 contains intermediate concentrations of the major ions, except for Ca, which is greater in the downflow water than in the upflow waters (see table 3 and figure 5). Mixing can produce the intermediate concentrations, and reactions with calcite can produce the observed increase in Ca concentration. Jarosite, which is supersaturated in both upflow and downflow waters can precipitate providing a sink for Fe, S, K, and Na.

Oxic and anoxic models were produced for comparison: "oxic" models included O_2 but excluded oxidized minerals (roemerite and pyrolusite), and "anoxic" included oxidized minerals. Six oxic models were generated that involved reactions with 1.39 to 2.23 mmol of O_2 and mixing of waters from wells 15A and 14 to produce the final downflow water (see table 5). Another 13 mixing models were generated which did not involve O_2, but which involved roemerite and pyrolusite. The mixing ratios for the oxic models (1-6) indicate that roughly 80 percent of the volume is from the zone represented by water of well 15A, and 20 percent is from that of well 14. The weighting of water from well 15A is consistent with conservative mixing of sulfate.

TABLE 5.--Summary of mass-transfer results[1]

WELL NAME AND MODEL[2]	MIXING RATIO	O_2 GAS	PYRITE	ROEMERITE	FERRI-HYDRITE	SODIUM JAROSITE	POTASSIUM JAROSITE	PYROLU-SITE	SIDERITE	CALCITE	CHLORITE	ILLITE	MICRO-CLINE	KAOLIN-ITE	SiO_2	CO_2 GAS
WELL 14B																
1	.	84.85	21.03	.	.	.	-15.04	.	27.33	3.87	.14	23.10	1.43	-27.69	-30.96	-28.55
2	.	32.87	7.16	.	-27.72	.	-1.17	.	27.33	3.84	1.30	.	1.43	-2.28	-4.40	-28.55
3	.	26.68	7.16	.	-3.81	.	-1.17	0.41	.	6.57	1.40	.	1.43	-2.39	-4.51	-3.95
4	.	33.82	9.07	.	.	.	-3.08	.41	.	6.57	1.24	3.17	1.43	-5.87	-8.15	-3.95
5	.	66.59	15.93	3.40	.	.	-16.74	.	27.33	3.84	.	25.93	1.43	-30.80	-34.22	-28.53
6	.	6.90	.	3.58	-31.30	.	-1.18	.	27.33	3.84	1.30	.	1.43	-2.28	-4.40	-28.55
7	.	8.84	.	11.36	-7.96	.	-16.74	.	27.33	3.84	.	25.93	1.43	-30.80	-34.22	-28.55
8	.	6.99	.	11.56	.	.	-17.14	.13	18.92	4.68	.	26.61	1.43	-31.58	-35.03	-20.98
9	.	1.33	.	6.05	.	.	-6.10	.41	.	6.57	1.00	8.21	1.43	-11.42	-13.95	-3.95
10	.	0.72	.	3.58	-7.96	.	-1.18	.41	.	6.57	1.41	1.43	1.43	-2.39	-4.51	-3.95
WELL 15B	**14B:14C**															
1	15:85	50.59	11.19	.	-55.05	.	-.26	.73	55.86	.	.	1.39	.26	.	-4.84	-56.26
2	15:85	10.03	.	5.59	-60.64	.	-.26	.73	55.86	.	.	1.39	.26	.	-4.84	-56.26
3	25:75	36.29	10.52	.	-5.82	.	-.15	.70	.	4.97	.	1.49	.13	.	-4.64	-5.61
4	25:75	.	.51	5.01	-10.82	.	-.15	.70	.	4.97	.	1.49	.13	.	-4.64	-5.61
5	33:67	33.89	9.88	.	-5.48	.	-.05	.66	.	4.97	.	1.36	.	.21	-4.24	-5.26
6	33:67	.	.52	4.68	-10.15	.	-.05	.66	.	4.38	.	1.36	.	.21	-4.24	-5.26
7	33:67	43.15	9.88	.	-43.82	.	-.05	.66	43.82	.	.	1.18	.	.39	-4.07	-44.70
8	33:67	7.35	.	4.94	-48.75	.	-.05	.66	43.82	.	.	1.18	.	.39	-4.07	-44.70
9	33:67	.	.	4.94	-18.30	.	-.05	.66	9.02	3.48	.	1.32	.25	.	-4.20	-13.37
10	23:77	.	.	5.31	-18.76	.	-.17	.70	8.66	4.20	.	1.47	.15	.	-4.68	-13.47
WELL 15A:																
1	.	3.46	1.05	2.08	.	-0.01	-.00	.	.80	.73	.11	.	.	1.37	-2.65	-1.53
2	.	.	.08	2.73	.	-.01	-.00	.	.80	.73	.09	.54	.	.78	-3.27	-1.53
3	.	.	.08	2.73	.	-.06	-.28	.	.80	.73	.11	.	.32	1.21	-3.29	-1.53
4	.	.	.13	2.55	.	-.01	-.00	.08	.27	.78	.11	.	.	1.37	-2.65	-1.06
WELL 1	**15A:14**															
1	80:20	1.39	.	.	.	-.70	-.91	.	2.17	.02	.	-5.66	5.09	3.17	-2.12	-2.49
2	80:20	1.39	.	.	.	-1.60	.	.	2.16	.02	.50	-15.73	11.13	11.22	-2.62	-2.49
3	79:21	1.41	.	.	-.44	-.68	-.82	.	2.43	.	.	-5.59	4.94	3.19	-1.94	-2.75
4	79:21	1.41	.	.	-.44	-1.49	.	.	2.43	.	.45	-14.68	10.39	10.47	-2.40	-2.75
5	79:21	2.23	.22	.	.	-.71	-1.00	.	2.43	.	.	-5.59	5.16	3.09	-2.38	-2.75
6	79:21	2.23	.22	.	.	-1.71	.	.	2.43	.	.56	-16.74	11.84	12.00	-2.94	-2.75
7	8:92	.	.32	3.77	.	-.24	-1.68	.31	.	.70	.	.72	1.43	.	-6.27	-2.15
8	15:85	.	.15	3.87	.	-.41	-2.26	.26	1.47	.51	.	.	2.63	.	-7.44	-3.32
9	16:84	.	.26	3.28	.	-.27	-1.48	.28	.	.64	.	.	1.71	.42	-5.52	-1.97
10	16:84	.	.32	2.39	-2.53	-.01	-.02	.28	.	.64	.	.	.	1.27	-2.10	-1.97
11	17:83	.	.32	2.36	-2.56	-.01	.	.28	.	.64	.	-.04	.	1.30	-2.03	-1.96
12	11:89	.	.	2.84	-7.94	-.02	-.03	.21	5.81	.10	.	.	.	1.45	-2.39	-7.31
13	12:88	.	.	2.79	-7.91	-.02	.	.21	5.74	.10	.	-.05	.	1.48	-2.30	-7.24
14	13:87	.	.	4.64	.	-.59	-3.29	.24	3.40	.32	.	.	3.84	-.55	-9.95	-5.09
15	13:87	.	.	4.15	-2.18	-.44	-2.40	.23	4.06	.26	.	.	2.79	.	-7.88	-5.70
16	21:79	.	.	3.95	.	-.56	-2.76	.22	2.72	.34	.	-.61	3.65	.	-8.43	-4.31
17	52:48	.	.	1.19	.	-.40	-.61	.14	.	.42	.	-3.05	2.87	2.19	-2.31	-1.18
18	52:48	.	.	1.19	.	-1.01	.	.14	.	.42	.34	-9.78	6.91	7.58	-2.64	-1.18
19	55:45	.	.	.69	-.93	-.32	.	.13	.	.40	.	-3.30	2.34	1.65	-.78	-1.11

[1] All mineral and gas mass-transfers are in millimoles per kilogram of water; negative for precipitation, positive for dissolution; no value for not reacted. Input data in table 3; mineral stoichiometry in table 4.

[2] Model flow paths shown in figure 7. Well name indicates "final" downflow water: well 14B <-- well 14C; well 15B <-- well 14B + well 14C; well 15A <-- well 15B; and well 15 <-- well 15A + well 14. Model number arbitrarily assigned to facilitate discussion of results.

However, mixing ratios for the anoxic models (7-19) range widely, indicating 8 to 55 percent of the volume is from the zone of well 15A. All 19 models involve reactions with relatively small quantities of pyrite and (or) larger quantities of roemerite plus carbonate and aluminosilicate minerals to produce the dissolved solutes and up to 4 mmol of jarosite. The argument for acid-generating reactions by ferric minerals under anoxic conditions is supported by the anoxic models; however, oxidized minerals such as roemerite and pyrolusite are not likely to occur along the deep flow path. Thus, the oxic mixing models may explain the hydrochemical trends in the deeper aquifer, even though the quantity of O_2 reacted exceeds the solubility maximum of 0.38 mmol/l. Errors in sulfate measurement are likely to cause the computed O_2 to be larger than actually is necessary to achieve mass balance. The error in the analytical charge balance for the samples (well 15A: +12 percent difference; well 15: +3 percent difference; and well 14: -1.23 percent difference) is greater in the high concentration range, suggesting that sulfate may be underestimated in waters from well 15A. A 3 percent error in the measured concentration sulfate in waters from well 15A (43 mmol/l), equates to 2.26 mmol of O_2 considering the stoichiometry of reaction 4. On the basis of this sulfate measurement error, any of the six oxic models (O_2 less than 2.23 mmol) could meet the closed system criteria. All six oxic models react siderite, microcline, and kaoline and produce jarosite, illite, silica, and CO_2. Model 1, which requires only 1.39 mmol of O_2 also involves the least mass transfer.

Discussion

Although DO concentrations were negligible in all samples, one cannot reject a mass-balance model that involves reaction with more O_2 than was measured, because the DO measurement indicates an instantaneous quantity in solution and does not indicate the integrated quantity of O_2 involved in geochemical reactions that produced the oxidized solutes in the water sample. The mass-transfer models indicate the integrated quantities of reactants and products. In an aqueous system closed to O_2, the saturation concentration of O_2 (0.38 mmol/l or less) is the maximum quantity of O_2 available for the integrated reactions, and the measured DO is the absolute limit of O_2 available for reactions downflow. Downflow increases in concentrations of sulfate indicate that sulfur-bearing minerals continued to decompose. Assuming that a closed system is in effect, one can reject mass-balance models that require extreme quantities of O_2 to generate the additional sulfate. Alternative, acceptable mass-balance models indicate that sulfate may be generated by reactions involving ferric-iron minerals (Fe^{3+} ions),

lesser quantities of pyrolusite (Mn^{4+} ions), and little or no O_2.

The roles of ferric ions and minerals in the oxidation of pyrite in open and closed systems are clearly important. Fe^{3+} is orders of magnitude more soluble than O_2 in acidic waters. The low pH (less than 3.5) and large quantities of SO_4^{2-} and Fe^{2+} in solution are compatible with the coupled ferric-iron reduction and sulfide-mineral oxidation reactions described by reactions 6 and 8. Thus, as demonstrated in the mass-balance models, SO_4^{2-} is likely to be generated under anoxic conditions in part by reactions with Fe^{3+} and FeS_2, and in part by dissolution of the previously formed ferric-sulfate minerals.

The timing and extent of formation of soluble ferric-sulfate minerals, such as roemerite, copiapite, and coquimbite in the mine spoil and unmined coal seams and the potential for sustained reactions between Fe^{3+} and pyrite is a question that has not been adequately addressed herein. The ferric-sulfate minerals are not the cause of AMD--they are intermediate products of pyrite oxidation. Oxygen must be available for these minerals to form and flowing water must be available to leach the oxidized solutes from the oxic zone(s). AMD formation cannot be prevented unless the oxidation of pyrite and (or) leaching of acid products are controlled. Different methods to remediate or prevent AMD will be necessary depending on whether oxidation products formed "acutely" during the transient effect of mining, or whether they form and leach "chronically" as a result of a continued O_2 convection and diffusion into the mine spoil and periodic leaching by recharge waters or a fluctuating ground water table. At this study site, and at others having similar hydrogeologic conditions, both acute and chronic formation of AMD is likely.

The precipitation of jarosite as a potential sink for Fe^{3+}, SO_4^{2-}, Na^+, and K^+ ions is suggested because it is supersaturated. In controlled systems, substantial quantities of Fe and S can be precipitated as jarosite if large concentrations of Na and (or) K are added (Norton et al. 1991). However, the subsurface precipitation of jarosite has not been confirmed and its supersaturation implies kinetic barriers to precipitation in natural systems (Nordstrom et al. 1979). Furthermore, the solubility of jarosite is such that relatively high concentrations of S and Fe can remain at equilibrium in solutions containing small concentrations of K and Na.

A potential benefit of reclamation with sewage sludge is the potential for stopping the formation of

AMD by excluding O_2 needed by T. ferrooxidans. Pulford et al. (1988) and Backes et al. (1988) provided laboratory evidence that the oxidation of pyrite can be inhibited by organic amendments such as chicken manure and wood waste. Decay of these organic materials consumes O_2, thus preventing the microbial oxidation of iron. However, the opposite trend is observed in comparing water-quality data for samples from nest 14 (unsludged) and nest 15 (sludged). Since the decay of organic matter also will produce CO_2 and release nutrients, it may provide sustenance for T. ferrooxidans. Nitrogen availability has been shown to limit growth of T. ferrooxidans in batch culture experiments (Lau et al. 1970), and ammonium, which predominates over nitrate in sewage sludge (Seaker and Sopper 1988a), is the essential nutrient form (Leathen et al. 1956; Silverman and Lundgren 1959). Thus, unless O_2 is depleted, sewage-sludge amendments could enhance the formation of AMD. At the study site, O_2 transport into the vadose zone was possible because sewage sludge was not spread over critical areas. Perhaps if sewage sludge had been spread over the entire recharge area, including the steep hillsides and toe of spoil, the transport of O_2 into the spoil and consequent oxidation of pyrite could have been reduced more effectively. However, even with more extensive coverage by sewage sludge, AMD can persist because of the presence of previously formed ferric-sulfate minerals and because of the presence of O_2 in recharge during winter months, when cold temperatures inhibit microbial decay of the sludge and soil organic matter.

Mass-transfer modeling is a useful procedure for quantifying the processes that cause water-quality changes and has provided insights into the potential causes and controls of AMD. However, geochemical modeling cannot substitute for basic data collection and hypothesis testing by statistical and other methods. Mass-transfer modeling assumes that the flow paths are well defined and that the stoichiometries of the reactants and products are known. Although the computations are precise, the models are simplified. The ground-water samples are from restricted points within broader flow "channels" defined by flow lines. The defined flow channels are not likely to contain the same water or solutes at upflow and downflow points because the flow of ground water is tortuous, and solutes will disperse. Furthermore, most mineral phases are impure and their stoichiometries are variable. This leads to two problems: (1) Thermodynamic data, which are needed to compute mineral SI's frequently are lacking for uncommon, impure, or amorphous minerals--for example, the necessary data are not available for roemerite, copiapite, or coquimbite. (2) The quantities of reactant and product minerals in a model depend on

their stoichiometries--certain phases indicated in the models may not exist along the flow path, and many different minerals may be reacted or produced to achieve the same mass-balance result.

Summary

Despite negligible concentrations of DO (less than 0.5 mg/l = 0.016 mmol/l), concentrations of dissolved sulfate and acidity increased in ground water from bedrock underlying the sewage-sludge-reclaimed mine spoil, suggesting that pyritic sulfur was oxidized below the water table. Furthermore, the waters beneath sewage-sludge-treated spoil were more acidic and contained substantially greater concentrations of dissolved minerals than those from beneath untreated spoil. This paper determined the predominant geochemical reactions that were likely to produce the highly mineralized water and evaluated if anoxic conditions limit oxidation of pyrite along potential ground-water flow paths.

In AMD, the oxidation of iron-sulfide minerals, produces dissolved acid, sulfate, and iron. Neutralization reactions with carbonate and silicate minerals produce elevated concentrations of manganese and aluminum, respectively, and additional dissolved solutes. Geochemical models for the oxidation of pyrite are presented to explain the potential role of O_2 and Fe^{3+} as oxidants under conditions open and closed to O_2, respectively, by reactions (1) and (6):

$$FeS_2 + 3.5\ O_2 + H_2O \Longrightarrow Fe^{2+} + 2\ SO_4^{2-} + 2\ H^+, \qquad (1)$$

$$FeS_2 + 14\ Fe^{3+} + 8\ H_2O \Longrightarrow$$
$$15\ Fe^{2+} + 2\ SO_4^{2-} + 16\ H^+. \qquad (6)$$
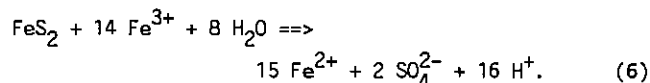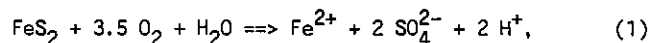
The iron-oxidizing bacteria, T. ferrooxidans, catalyze the oxidation of Fe^{2+} to Fe^{3+} in oxic systems and increase the rate of pyrite oxidation by reaction 6. Reactions (1) and (6) can occur in oxic systems above the water table, whereas reaction (6) also can occur in anoxic systems below the water table. Secondary minerals such as roemerite [$Fe^{2+}Fe_2^{3+}(SO_4)_4 \cdot 14H_2O$], copiapite [$Fe^{2+}Fe_4^{3+}(SO_4)_6(OH)_2 \cdot 20H_2O$], and coquimbite [$Fe_2(SO_4)_3 \cdot 9H_2O$], which were identified with FeS_2 in coal samples, form on the oxidizing surface of pyrite and precipitate as efflorescences above the water table. These soluble ferric-sulfate "salts" are a source of SO_4^{2-} and Fe^{3+}, which can dissolve in recharge waters, or in ground water during a water-table rise, and can be transported to pyrite reaction sites where DO is absent. For example, the dissolution of roemerite and oxidation of pyrite does not involve O_2

$$FeS_2 + 7\ Fe^{2+}Fe_2^{3+}(SO_4)_4 \cdot 14H_2O \Longrightarrow$$
$$22\ Fe^{2+} + 30\ SO_4^{2-} + 16\ H^+ + 90\ H_2O. \qquad (8)$$
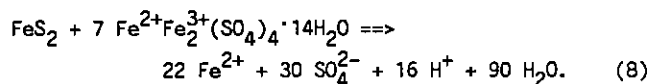
The computer programs WATEQ4F and NEWBAL were used to compute chemical equilibrium and mass transfer, respectively, considering mineral dissolution and precipitation reactions plus mixing of waters from different upflow zones. Mass-balance models indicate that (a) extremely large quantities of O_2, greater than 100 times its aqueous solubility, can generate observed concentrations of dissolved SO_4^{2-} from FeS_2, and (b) under anoxic conditions, Fe^{3+} from dissolved ferric-sulfate minerals can oxidize FeS_2 along closed-system ground-water flow paths. In a system open to O_2, such as in the unsaturated zone, the aqueous solubility of O_2 is not limiting, and oxidation of FeS_2 by O_2 and Fe^{3+} accounts for most SO_4^{2-} and Fe^{3+} observed in acidic ground water. However, in a system closed to O_2, such as in the saturated zone, O_2 solubility is limiting; hence, ferric oxidation of pyrite is a reasonable explanation for the observed increase in concentration of SO_4^{2-} with increasing depth below the water table.

Conclusions

Mining has disturbed the landscape and has induced changes in the hydrologic system that have promoted the oxidation of pyrite and formation of AMD. Use of sewage sludge in surface-mine reclamation helps to dispose of sludge and to revegetate barren spoil. However, there is still some question regarding potential beneficial effects of the sludge on local ground-water quality. Acidic ground water beneath sludge-treated spoil results from a combination of factors, including: (1) dissolution of pyrite and ferro-ferric-sulfate minerals; (2) lateral flow of gaseous and dissolved O_2 (reactants) into the mine spoil from permeable, unsludged zones; and (3) potential for increased growth of $\underline{T}.\ \underline{ferrooxidans}$, which require O_2 plus CO_2 and nutrients provided by sludge.

DO concentrations are neglible in all the ground water measured, whether from sewage-sludge-treated or untreated zones through mine spoil or bedrock. This implies that the application of sewage sludge did not cause the depletion of DO. Furthermore, the mineralization of the water beneath sludge-treated spoil suggests local addition of sludge did not inhibit, and may have enhanced, the production of acid. The aerobic decomposition of sludge generates carbon dioxide as DO is consumed. Nitrate, ammonium, and phosphate nutrients are likely to be leached and may be utilized by $\underline{T}.$ $\underline{ferrooxidans}$ in the mine spoil and bedrock. If the bacteria utilize the nutrients, then the concentrations will be reduced and the effect of nutrient leaching will not be obvious by the measurement of dissolved nitrogen or phosphorus concentrations; the bacteria also should be enumerated.

The objective of identifying the reactants and products that control water chemistry cannot be achieved by modeling of water-quality data alone. Hydrological, mineralogical, and rock-chemical data are critically important for describing the geochemical evolution of acidic ground water. Missing data on heat and gaseous fluxes, pyrite distribution, and recharge infiltration through the unsaturated mine spoil would help to define the potential for oxidation of pyrite above the water table. The location and timing of production of ferric-sulfate minerals are uncertain and have not been adequately addressed herein. The inorganic sulfur to iron (Sin/Fe) ratios in rock-core subsamples are compatible with the mineral formulas for pyrite, roemerite, copiapite, and coquimbite, which were found in high-sulfur coal samples collected from a zone that is presently below the water table. Little information exists on the subsurface formation and occurrence of the "sulfate-salts," especially under saturated conditions. Such salts are important as sinks or sources of AMD by providing storage in a solid phase during "dry" periods and by providing an active oxidizing agent when dissolved during "wet" periods.

There are practical implications for the open- and closed-system scenarios for pyrite oxidation and the observed increasing mineralization of ground water with increasing depth below the water table. For example, "special handling" involves the segregation of pyritic materials during surface-coal mining and the subsequent placement of isolated pods of the toxic spoil within the mine backfill. The intent is to prevent reactions that produce acid and prevent the transport of acid from the isolation zones. The PaDER encourages concurrent mining and reclamation with placement of the toxic spoil above the water table--thereby reducing pyrite exposure to air during mining, but increasing its exposure after reclamation. However, others argue that pyritic materials should be placed below the water table where O_2 solubility constraints will limit the extent of acid-forming oxidation reactions (Hammack and Watzlaf 1990). On the basis of results presented herein, neither placement technique is ideal: It is likely that placement of pyrite above the water table will allow the oxidation of pyrite by humid, oxygenated air within the unsaturated zone, and that the placement of pyrite below the water table will allow the oxidation of pyrite both by DO (open system?) and Fe^{3+} ions. Thus unless the material is tightly encapsulated, acid-forming reactions are likely to occur both above and below the water

table. Further study of the problem concerning oxidation of pyrite above and below the water table is necessary to establish the feasibility and success of special-handling techniques.

Additional efforts can be made to establish the mechanisms and rates of acid-forming reactions:

(1) To test if pyrite is oxidized by O_2 or Fe^{3+} ions by reactions (1) or (6), respectively, oxygen isotopes in SO_4, H_2O, and O_2 molecules can be measured. The oxygen atoms in SO_4 should have $d^{18}O$ between atmospheric O_2 ($d^{18}O \cong +23^o/oo$) and meteoric H_2O ($d^{18}O \cong -10^o/oo$) (Taylor et al. 1984a,b), and will approach the meteoric water composition if the ferric-iron oxidation predominates.

(2) To determine if sewage sludge enhances the growth of _T. ferrooxidans_, ground waters from sludge-treated and untreated mine spoil can be chemically analyzed and bacteria can be enumerated.

(3) To compute kinetics of pyrite oxidation "in the field," ground-water flow velocities can be determined using a calibrated numerical model coupled with the geochemical mass-transfer results.

Literature Cited

Backes, C. A.; I. D. Pulford; and H. J. Duncan 1988. Treatments to combat pyrite oxidation in coal mine spoil. U.S. Bureau of Mines Information Circular 9183 1:91-96.

Baker, J. P. and C. L. Schofield 1982. Aluminum toxicity to fish in acidic waters. Water, Air, and Soil Pollution 18:289-309.

Baker, R. A. (Mellon Institute) 1971. Evaluation of pyritic oxidation by nuclear methods. U.S. Environmental Protection Agency Water Pollution Control Research Report 14010--F1103/71.

Ball, J. W.; D. K. Nordstrom; and D. W. Zachman 1987. WATEQ4F--A personal computer FORTRAN translation of the geochemical model WATEQ2 with revised data base. U.S. Geological Survey Open-File Report 87-50, 108 p.

Barnes, Ivan and F. E. Clarke 1964. Geochemistry of ground water in mine drainage problems. U.S. Geological Survey Professional Paper 473-A, p. A1-A5.

Berg, T. M. and others 1980. Geologic map of Pennsylvania. Pennsylvania Geological Survey, Fourth Series, Map 1, scale 1:2,500,000, 3 sheets.

Berg, T. M.; M. K. McInerney; J. H. Way; and D. B. MacLachlan 1983. Stratigraphic correlation chart of Pennsylvania. Pennsylvania Geological Survey, Fourth Series, General Geology Report 75.

Blickwedel, R. S. and J. H. Linn 1987. Hydrogeology and ground-water quality at a land reclamation site, Neshaminy State Park, Pennsylvania. U.S. Geological Survey Water-Resources Investigations Report 86-4164, 41 p.

Brady, K. B. C. and R. J. Hornberger 1989. Mine drainage prediction and overburden analysis in Pennsylvania. Proceedings Annual West Virginia Surface Mine Drainage Task Force Symposium, April 25-26, 1989, Morgantown, W.V., 13 p.

Buckwalter, T. F; C. H. Dodge; G. R. Schiner; and H. E. Koester 1981. Water resources of the Clarion River and Redbank Creek basins, northwestern Pennsylvania. U.S. Geological Survey Open-File Report 81-70, 111 p.

Burrows, W. D. 1977. Aquatic aluminum--chemistry, toxicology, and environmental prevalence. CRC Critical Reviews in Environmental Controls 7:167-216. http://dx.doi.org/10.1080/10643387709381651

Burton, T. M. and J. W. Allan 1986. Influence of pH, aluminum, and organic matter on stream invertebrates. Canadian Journal of Fisheries and Aquatic Sciences 43:1285-1289. http://dx.doi.org/10.1139/f86-159

Cathles, L. M. 1982. Acid mine drainage. The Pennsylvania State University Earth and Mineral Sciences 51(4):37-41.

Champ, D. R.; R. L. Gulens; and R. E. Jackson 1979. Oxidation reduction sequences in ground water flow systems. Canadian Journal of Earth Science 16:12-23. http://dx.doi.org/10.1139/e79-002

Colmer, A. R. and M. E. Hinkle 1947. The role of microorganisms in acid mine drainage--A preliminary report. Science 106(2747):253-256. http://dx.doi.org/10.1126/science.106.2751.253

Colmer, A. R.; K. L. Temple; and M. E. Hinkle 1949. An iron-oxidizing bacterium from the drainage of some bituminous coal mines. Journal of Bacteriology 59:317-328.

Cravotta, C. A. III; K. B. C. Brady; M. W. Smith; and R. L. Beam 1990. Effectiveness of the addition of alkaline materials at surface coal mines in preventing or abating acid mine drainage--1. Geochemical considerations. Proceedings of the 1990 Mining and Reclamation Conference and Exhibition, Charleston, West Virginia, April 23-26, 1990 1:221-225.
https://doi.org/10.21000/JASMR90010221

Davis, Alan 1981. Sulfur in coal. The Pennsylvania State University Earth and Mineral Sciences 51(2):13-21.

Dixon, J. B.; L. R. Hossner; A. L. Senkayi; and K. Egashira 1982. Mineralogical properties of lignite overburden as they relate to mine spoil reclamation, in Kittrick, J. A.; D. S. Fanning; and L. R. Hossner, eds., Acid sulfate weathering. Soil Science Society of America, p. 169-191.

Drever, J. I. 1982. The geochemistry of natural waters. Englewood Cliffs, N.J., Prentice-Hall, Inc., 388 p.

Gang, M. W. and D. Langmuir 1974. Controls on heavy metals in surface and ground waters affected by coal mine drainage--Clarion River and Redbank Creek watershed, Pennsylvania. National Coal Association/ Bituminous Coal Research Inc., 5th Symposium on Coal Mine Drainage Research, Louisville, Ky., p. 39-69.

Garrels, R. M. and M. E. Thompson 1960. Oxidation of pyrite in ferric sulfate solution. American Journal of Science, 258:57-67.

Hammack, R. W. and G. R. Watzlaf 1990. The effect of oxygen on pyrite oxidation. Proceedings of the 1990 Mining and Reclamation Conference and Exhibition, Charleston, West Virginia, April 23-26, 1990, v. 1, p. 257-264.
https://doi.org/10.21000/JASMR90010257

Harbaugh, A. W. 1990. A simple contouring program for gridded data. U.S. Geological Survey Open-File Report 90-144, 12 p.

Hawkins, J. W. 1984. Iron disulfide characteristics of the Waynesburg, Redstone, and Pittsburgh coals in West Virginia and Pennsylvania. Morgantown, W.V., West Virginia University, M.S. thesis, 195 p.

Hem, J. D. 1985. Study and interpretation of the chemical characterisics of natural water (3d). U.S. Geological Survey Water-Supply Paper 2254, 263 p.

Henke, J. R. 1985. Hydrogeologic characterization of a surface mining-impacted watershed with implications for acid mine drainage abatement, Clarion County, Pennsylvania. Pennsylvania State University, unpublished M.S. thesis, 171 p.

Jaynes, D. B.; H. B. Pionke; and A. S. Rogowski 1984a. Acid mine drainage from reclaimed coal strip mines--2. Simulation results of model. Water Resources Research 20(2):243-250.

Jaynes, D. B.; A. S. Rogowski; and H. B. Pionke 1984b. Acid mine drainage from reclaimed coal strip mines--1. Model description. Water Resources Research 20(2):233-242.

Karathanasis, A. D.; V. P. Evangelou; and Y. L. Thompson 1988. Aluminum and iron equilibria in soil solutions and surface waters of acid mine watersheds. Journal of Environmental Quality 17:534-543.
doi:10.2134/jeq1988.00472425001700040003x

Karathanasis, A. D.; Y. L. Thompson; and V. P. Evangelou 1990. Temporal solubility trends of aluminum and iron leached from coal spoils and contaminated soils. Journal of Environmental Quality 19:389-395.
http://dx.doi.org/10.2134/jeq1990.00472425001900030007x

Kleinmann, R. L. P.; D. A. Crerar; and R. R. Pacelli 1980. Biogeochemistry of acid mine drainage and a method to control acid formation. Mining Engineering 33:300-306.

Lau, C. M.; K. S. Shumate; and E. E. Smith 1970. The role of bacteria in pyrite oxidation kinetics. Third symposium on coal mine drainage research, Pittsburgh, Pennsylvania, May 19-20, 1970, p. 114-121.

Leathen, W. W.; N. A. Kinsel; and S. A. Braley 1956. Ferrobacillus ferrooxidans--A chemosynthetic, autotrophic bacterium. Journal of Bacteriology 72:700-704.

McDonald, M. G. and A. W. Harbaugh 1988. A modular three-dimensional finite-difference ground-water flow model. U.S. Geological Survey Techniques of Water-Resources Investigations TWRI 6-A1, 586 p.

McKibben, M. A. and H. L. Barnes 1986. Oxidation of pyrite in low temperature acidic solutions--Rate laws and surface textures. Geochimica et Cosmochimica Acta 50:1509-1520.
http://dx.doi.org/10.1016/0016-7037(86)90325-X

Morrison, J. L.; S. D. Atkinson; A. Davis; and B. E. Scheetz 1990a. The use of CO_2 coulometry in differentiating and quantifying the carbonate phases in the coal-bearing strata of western Pennsylvania--its applicability in interpreting and modifying neutralization potential (NP) measurements. [Proceedings of the 1990 Mining and Recla]mation Conference and Exhibition, Charleston, West Virginia, April 23-26, 1990, v. 1, p. 243-248.
http://dx.doi.org/10.21000/JASMR90010249

http://dx.doi.org/10.21000/JASMR90010243
Morrison, J. L.; S. D. Atkinson; and B. E. Scheetz 1990b. Delineation of potential manganese sources in the coal and overburdens of western Pennsylvania. Proceedings of the 1990 Mining and Reclamation Conference and Exhibition, Charleston, West Virginia, April 23-26, 1990, v. 1, p. 249-256.

Moses, C. O.; D. K. Nordstrom; J. S. Herman; and A. L. Mills 1987. Aqueous pyrite oxidation by dissolved oxygen and by ferric iron. Geochimica et Cosmochimica Acta 51:1561-1571.
http://dx.doi.org/10.1016/0016-7037(87)90337-1

Mozley, P. S. 1989. Relationship between depositional environment and the elemental composition of early diagenetic siderite. Geology 17:704-706.
http://dx.doi.org/10.1130/0091-7613(1989)017<0704:RBDE

National Oceanic and Atmospheric Administration 1987. Climatological data annual summary, Pennsylvania 1987. NOAA 92:(13) Clarion 3 SW.

National Oceanic and Atmospheric Adminsitration 1988. Climatological data annual summary, Pennsylvania 1988. NOAA 93:(13) Clarion 3 SW.

Noll, D. A.; T. W. Bergstresser; and J. Woodcock 1988. Overburden sampling and testing manual. Pennsylvania Department of Environmental Resources Bureau of Mining and Reclamation, 78 p.

Nordstrom, D. K. 1982. Aqueous pyrite oxidation and the consequent formation of secondary iron minerals, in Kittrick, J. A.; D. S. Fanning; and L. R. Hossner, eds., Acid sulfate weathering. Soil Science Society of America, p. 37-63.

Nordstrom, D. K.; E. A. Jenne; and J. W. Ball 1979. Redox equilibria of iron in acid mine waters, in Jenne, E. A., ed., Chemical modeling in aqueous systems--Speciation, sorption, solubility, and kinetics. American Chemical Society Symposium Series 93, p. 51-79.

Norton, G. A.; R. G. Richardson; R. Markuszewski; and A. D. Levine 1991. Precipitation of jarosite compounds as a method for removing impurities from acidic wastes from chemical coal cleaning. Environmental Science and Technology 25:449-455.
http://dx.doi.org/10.1021/es00015a011

Palache, Charles; H. Berman; and C. Frondel 1951. System of mineralogy (7th). New York, John Wiley and Sons, 1124 p.

Parkhurst, D. L.; L. N. Plummer; and D. C. Thorstenson 1982. BALANCE--a computer program for calculating mass transfer for geochemical reactions in ground water. U.S. Geological Survey Water-Resources Investigations Report 82-14, 29 p.

Plummer, L. N. and W. Back 1980, The mass balance approach--application to interpreting the chemical evolution of hydrologic systems. American Journal of Science 280:130-142.
http://dx.doi.org/10.2475/ais.280.2.130

Plummer, L. N.; J. F. Busby; R. W. Lee; and B. B. Hanshaw 1990. Geochemical modeling of the Madison aquifer in parts of Montana, Wyoming, and South Dakota. Water Resources Research 26:1981-2014.
http://dx.doi.org/10.1029/WR026i009p01981

Plummer, L. N.; D. L. Parkhurst; and D. C. Thorstenson 1983. Development of reaction models for groundwater systems. Geochimica et Cosmochimica Acta 47:665-685.

Pollack, D. W. 1989. Documentation of computer programs to compute and display pathlines using results from the U.S. Geological Survey modular three-dimensional finite-difference ground-water flow model. U.S. Geological Survey Open-File Report 89-381, 188 p.

Pulford, I. D.; C. A. Backes; and H. J. Duncan 1988. Inhibition of pyrite oxidation in coal mine waste, in Selected papers of the Dakar symposium on acid sulphate soils, Dakar, Senegal, January, 1986. Netherlands, International Institute for Land Reclamation and Improvement, ILRI 44, p. 59-67.

Saad, D. A. and C. A. Cravotta III 1991. Modeling of ground-water flow along a cross section through a reclaimed surface coal mine in western Pennsylvania (abs.). American Association of Surface Mining and Reclamation, 8th Annual National Meeting, May 14-17, 1991, Durango, Co.

Seaker, E. M. and W. E. Sopper 1988a. Municipal sludge for minespoil reclamation--I. Effects on microbial populations and activity. Journal of Environmental Quality 17(4):591-597.
http://dx.doi.org/10.2134/jeq1988.00472425001700040012x

Seaker, E. M. and W. E. Sopper 1988b. Municipal sludge for minespoil reclamation--II. Effects on organic matter. Journal of Environmental Quality 17(4):598-602.

http://dx.doi.org/10.2134/jeq1988.00472425001700040013x

Senkayi, A. L.; J. B. Dixon; and L. R. Hossner 1986. Todorokite, goethite, and hematite--alteration products of siderite in east Texas lignite overburden. Soil Science 142:36-42.

http://dx.doi.org/10.1097/00010694-198607000-00006

Skougstad, M. W.; M. J. Fishman; L. C. Friedman; and others 1979. Methods for the determination of inorganic substances in water and fluvial sediments. U.S. Geological Survey Techniques of Water-Resources Investigations TWRI 5-A1, 626 p.

Silverman, M. P. and D. G. Lundgren 1959. Studies on the chemolithotrophic iron bacterium Ferrobacillus ferrooxidans--1. An improved medium and a harvesting procedure for securing high cell yields. Journal of Bacteriology 77:642-647.

Singer, P. C. and W. Stumm 1970a. Acidic mine drainage--the rate-determining step. Science 167:1121-1123.

http://dx.doi.org/10.1126/science.167.3921.1121

Singer, P. C. and W. Stumm (Harvard University) 1970b. Oxygenation of ferrous iron. U.S. Department of the Interior, Federal Water Quality Administration (U.S. Environmental Protection Agency) Water Pollution Control Research Report 14010--067/69.

Sobek, A. A.; W. A. Schuller; J. R. Freeman; and R. M. Smith 1978. Field and laboratory methods applicable to overburdens and minesoils. Cincinatti, Ohio, U.S. Environmental Protection Agency Environmental Protection Technology EPA-600/2-78-054, 203 p.

Sopper, W. E. and E. M. Seaker 1984. Strip mine reclamation with municipal sewage sludge. U.S. Environmental Protection Agency EPA-600/S2-84-035.

Stumm, Werner and J. J. Morgan 1981. Aquatic chemistry--an introduction emphasizing chemical equilibria in natural waters (2nd). New York, John Wiley and Sons, 780 p.

Taylor, B. E.; M. C. Wheeler; and D. K. Nordstrom 1984a. Oxygen and sulfur isotope compositions of sulfate in acid mine drainage--evidence for oxidation mechanisms. Nature 308:538-541.

http://dx.doi.org/10.1038/308538a0

Taylor, B. E.; M. C. Wheeler; and D. K. Nordstrom 1984b. Stable isotope geochemistry of acid mine drainage--experimental oxidation of pyrite. Geochimica et Cosmochimica Acta 48:2669-2678.

Temple, K. L and A. R. Colmer 1951. The autotrophic oxidation of iron by a new bacterium, Thiobacillus ferrooxidans. Journal of Bacteriology 62:605-611.

Temple, K. L. and E. W. Delchamps 1953. Autotrophic bacteria and the formation of acid in bituminous coal mines. Applied Microbiology 1:255-258.

Temple, K. L. and W. A. Koehler 1954. Drainage from bituminous coal mines. West Virginia University Bulletin (Series 54, No. 4-1) Engineering Experiment Station Research Bulletin 25, 35 p.

Whittemore, D. O. and D. Langmuir 1975. The solubility of ferric oxyhydroxides in natural waters. Ground Water 13:360-365.

Williams, E. G. 1960. Marine and fresh water fossilferous beds in the Pottsville and Allegheny Groups of western Pennsylvania. Journal of Paleontology 34:908-922.

Wood, W. W. 1976. Guidelines for collection and field analysis of ground-water samples for selected unstable constituents. U.S. Geological Survey Techniques of Water-Resources Investigations TWRI 1-D2, 24 p.

Zajic, J. E. 1969. Microbial biogeochemistry. New York, Academic Press, 345 p.